

# Acceleration of primary and secondary particles in galaxy clusters by compressible MHD turbulence : from radio halos to gamma rays

G. Brunetti,<sup>1</sup> A. Lazarian<sup>2</sup>

<sup>1</sup> *INAF/Istituto di Radioastronomia, via Gobetti 101, I-40129 Bologna, Italy*

<sup>2</sup> *Department of Astronomy, University of Wisconsin at Madison, 5534 Sterling Hall, 475 North Charter Street, Madison, WI 53706, USA*

19 October 2018

## ABSTRACT

Radio observations discovered large scale non thermal sources in the central Mpc regions of dynamically disturbed galaxy clusters (radio halos). The morphological and spectral properties of these sources suggest that the emitting electrons are accelerated by spatially distributed and gentle mechanisms, providing some indirect evidence for turbulent acceleration in the inter-galactic-medium (IGM).

Only deep upper limits to the energy associated with relativistic protons in the IGM have been recently obtained through gamma and radio observations. Yet these protons should be (theoretically) the main non-thermal particle component in the IGM implying the unavoidable production, at some level, of secondary particles that may have a deep impact on the gamma ray and radio properties of galaxy clusters.

Following Brunetti & Lazarian (2007), in this paper we consider the advances in the theory of MHD turbulence to develop a comprehensive picture of turbulence in the IGM and extend our previous calculations of particle acceleration by compressible MHD turbulence by considering self-consistently the reacceleration of both primary and secondary particles. Under these conditions we expect that radio to gamma ray emission is generated from galaxy clusters with a complex spectrum that depends on the dynamics of the thermal gas and Dark Matter. The non-thermal emission results in very good agreement with radio observations and with present constraints from hard X-ray and gamma ray observations. In our model giant radio halos are generated in merging (turbulent) clusters only. However, in case secondaries dominate the electron component in the IGM, we expect that the level of the Mpc-scale synchrotron emission in more relaxed clusters is already close to that of the radio upper limits derived by present observations of clusters without radio halos. Important constraints on cluster physics from future observations with present and future telescopes are also discussed.

**Key words:** acceleration of particles - turbulence - radiation mechanisms: non-thermal - galaxies: clusters: general - radio continuum: general - X-rays: general

## 1 INTRODUCTION

Radio observations of galaxy clusters prove the presence of non-thermal components, magnetic fields and relativistic particles, mixed with the hot Inter-Galactic-Medium (IGM) (e.g. Ferrari et al, 2008).

Potentially, cluster mergers can be responsible for the origin of the non-thermal components in IGM. During these events a fraction of the gravitational binding-energy of Dark Matter halos that is converted into internal energy of the baryonic matter can be channelled into the amplification of the magnetic fields (e.g. Dolag et al. 2002; Subramanian et al. 2006; Ryu et al. 2008) and into the acceleration of par-

ticles via shocks and turbulence (e.g. Ensslin et al 1998; Sarazin 1999; Blasi 2001; Brunetti et al. 2001, 2004; Petrosian 2001; Miniati et al. 2001; Fujita et al 2003; Gabici & Blasi 2003; Ryu et al. 2003; Cassano & Brunetti 2005; Hoeft & Bruggen 2007; Brunetti & Lazarian 2007; Pfrommer 2008).

Theoretically relativistic protons are expected to be the dominant non-thermal particles component since they have long life-times and remain confined within galaxy clusters for a Hubble time (Völk et al. 1996; Berezhinsky, Blasi & Ptuskin 1997; Ensslin et al 1998). Proton-proton collisions in the IGM inject secondary particles, including neutral pions that

decay into gamma rays and relativistic electrons that produce synchrotron and inverse Compton (IC) emission. So far only upper limits to the gamma ray emission from galaxy clusters have been obtained by FERMI and Cherenkov telescopes (eg., Aharonian et al 2009a,b; Aleksic et al 2010; Ackermann et al 2010). These upper limits, together with constraints from complementary approaches based on radio observations (eg., Reimer et al 2004; Brunetti et al. 2007) suggest that relativistic protons contribute to less than a few percent of the energy of the IGM, at least in the central Mpc-sized regions.

Relativistic electrons in the IGM are nowadays studied by radio observations of diffuse synchrotron radiation from galaxy clusters. Radio halos are the most spectacular examples of cluster-scale radio sources, they are diffuse radio sources that extend on Mpc-scales in the cluster central regions and are found in about 1/3 of massive galaxy clusters (eg. Feretti 2002; Ferrari et al. 2008; Cassano 2009).

The origin of relativistic electrons in radio halos is still debated. In the context of the *hadronic* model (Dennison 1980; Blasi & Colafrancesco 1999; Pfrommer & Ensslin 2004) radio halos are due to synchrotron emission from secondary electrons generated by p-p collisions, in which case clusters are (unavoidably) gamma ray emitters due to the decay of the  $\pi^0$  produced by the same collisions. The very recent non-detections of nearby galaxy clusters at GeV energies by FERMI significantly constrain the role of secondary electrons in the non-thermal emission (Ackermann et al 2010). Similarly, previous works pointed out that the spectral and morphological properties of a number of radio halos appear inconsistent with a simple hadronic origin of the emitting particles (eg. Brunetti et al 2008, 2009; Donnert et al 2010a,b; Macario et al 2010).

A second scenario proposed for the origin of radio halos is based on turbulent reacceleration of relativistic particles in connection with cluster-mergers events (eg., Brunetti et al. 2001; Petrosian 2001; Berrington & Dermer 2003; Fujita et al 2003; Cassano & Brunetti 2005). The acceleration of thermal electrons to relativistic energies by MHD turbulence in the IGM faces serious drawbacks based on energy arguments (eg., Petrosian & East 2008), consequently in these models it must be assumed a pre-existing population of relativistic electrons in the cluster volume that provides the seed particles to reaccelerate during mergers. These seeds may be primary electrons injected by SN, AGN, galaxies and shocks in the cluster volume that can be accumulated for a few Gyrs at energies of a few hundred MeV (eg., Sarazin 1999; Brunetti et al 2001).

MHD turbulence theory seriously advanced in the last decades also affecting our view of particle acceleration in astrophysical plasmas (e.g. Chandran 2000; Yan & Lazarian 2002; Lazarian 2006a and ref therein). For this reason in Brunetti & Lazarian (2007) we considered the advances in the theory of MHD turbulence to develop a comprehensive picture of turbulence in the IGM and to study the reacceleration of relativistic particles. In this respect, our main conclusions were that the compressible MHD turbulence (essentially fact modes), generated in connection with energetic cluster-mergers, is the most important source of stochastic particle reacceleration in the IGM and that the interaction between this turbulence and the relativistic electrons may

explain the origin of radio halos, provided that enough seed relativistic electrons are accumulated in the IGM.

At the same time relativistic protons should be accumulated (at some level) in the IGM and consequently MHD turbulence may also reaccelerate these protons and their secondary products (Brunetti & Blasi 2005). On one hand, in this case secondaries come into the picture as a natural pool of seed particles, on the other hand the reacceleration of relativistic protons is expected to enhance the production rate of these secondaries with the possible drawback that this would overcome the effect of reacceleration, thus making the overall picture unsustainable.

Previous papers addressed this problem and model turbulent reacceleration of both primary and secondary particles in the IGM in the context of cluster-mergers driven turbulence (Brunetti & Blasi 2005; Brunetti et al 2009a). These papers explored the complex non-thermal spectrum from galaxy clusters that is expected in this situation and first predicted the interplay of a long-living spectral component, due to relativistic protons and their chain of secondary particles, with a transient emission, leading to the formation of radio halos, that is due to the reacceleration of electrons in cluster mergers. Remarkably, in this general situation gamma ray emission is expected from galaxy clusters, although at a lower level than that expected from the pure hadronic case (eg. Brunetti et al 2009a)\*.

All these papers addressing the reacceleration of primary and secondary particles focus on Alfvénic reacceleration and assume the injection of Alfvén modes at small, resonant, scales, in which case however it is difficult to derive a overall self-consistent picture connecting clusters mergers and the generation of these modes at such small scales. This makes necessary an exploration of this picture in the context of a more comprehensive model of MHD turbulence in clusters, that is the goal of our paper.

Our study is also timely due to the recent gamma and radio observations that put severe constraints to the energy density of the relativistic proton component in galaxy clusters (Brunetti et al 2007; Aharonian et al 2009a,b; Aleksic et al 2010; Ackermann et al 2010), and that allows for including this component in models with substantially less degree of freedom than in the past.

For these reasons, in this paper we extend our calculations presented in Brunetti & Lazarian (2007) by considering self-consistently relativistic protons, the generation of secondary particles in the IGM and their reacceleration by MHD turbulence generated in cluster mergers.

In Section 2 we discuss the properties of turbulence in galaxy clusters, in Sect.3 we summarize the formalism for particle acceleration and evolution, in Sect.4 we first discuss the connection between mergers and particle reacceleration by turbulence and then show our results, and in Sect.5 we give our conclusions and discuss model simplifications, future extensions of the work and a comparison with previous works.

A  $\Lambda$ CDM cosmology with  $H_0 = 70$  km/s/Mpc,  $\Lambda = 0.7$  and  $\Omega_0 = 0.3$  is assumed.

\* assuming the same cluster magnetic field and for a given synchrotron luminosity

## 2 TURBULENCE IN THE IGM

Numerical simulations of galaxy clusters suggest that turbulent motions may store an appreciable fraction, 5–30%, of the thermal energy of the IGM (e.g., Roettiger, Burns, Loken 1996; Roettiger, Loken, Burns 1997; Ricker & Sarazin 2001; Sunyaev, Bryan & Norman 2003; Dolag et al. 2005; Vazza et al. 2006, 2009a; Paul et al 2010). The largest turbulent eddies should decay into a turbulent velocity field on smaller scales, possibly developing a turbulent cascade.

It is known that the mean free path of thermal protons arising from Coulomb collisions in the hot IGM may be very large, ten to hundred kpc. Fluids in such a collisionless regime can be very different from their collisional counterparts (Schekochihin et al. 2005; 2010). The parallel to magnetic field viscosity of IGM can be very large and the collisionless plasmas are subject to various instabilities. Those, however, we believe change the effective collisionality of the fluid, justifying the application of MHD to describing the IGM at least on its large scales (see Lazarian et al. 2010). Indeed, particles in plasmas can interact through the mediation of the perturbed magnetic fields, and effective collisionality of plasmas may differ dramatically from the textbook estimates. The difference stems from the very instabilities that are present in the IGM plasmas (firehose, mirror, gyroresonance etc.). These instabilities are expected to transfer the energy from the turbulent compressions on the scales less or equal to the particle mean free path to the perturbations at the particle gyroscale. This has been described in Lazarian & Beresnyak (2006), as a result of the scattering, the mean free path of particles decreases, which makes the fluid essentially collisional over a wide range of scales, with the critical scale for which the fluid gets effectively collisional that is expected to decrease with the increase of turbulent driving rate. While some parts of the aforementioned paper dealing with the interaction of turbulence and cosmic rays remain controversial, a similar approach should be reliably applicable to thermal plasma particles. Therefore we believe that on scales much larger than the thermal particle gyroradius the turbulence can be treated in the MHD approximation and shall apply below the theory of MHD turbulence to the IGM.

Turbulence generated during cluster mergers is expected to be injected at large scales,  $L_o \sim 100 - 400$  kpc, with typical velocity of the turbulent eddies at the injection scale around  $V_o \sim 300 - 700$  km/s (eg. Subramanian et al 2006). This makes turbulence sub-sonic, with  $M_s = V_o/c_s \approx 0.25 - 0.6$ , but strongly super-Alfvénic, with  $M_A = V_o/v_A \approx 5 - 10$ . Turbulent motions at large scales are thus essentially hydrodynamics and the cascading of compressive (magnetosonic) modes may couple with that of solenoidal motions (Kolmogorov eddies).

In Brunetti & Lazarian (2007) we discussed that the important consequence of the turbulence in magnetized plasma is that both solenoidal and compressive modes in hot galaxy clusters would not be strongly affected by viscosity at large scales and an inertial range is established, provided that the velocity of the eddies at large scales exceeds  $\approx 300$  km/s. In the Kolmogorov cascade the turbulent velocity  $V_l$  scales as  $V_L(l/L_o)^{1/3}$ , and at scales less than  $l_A \sim L_o M_A^{-3}$  the turbulence gets sub-Alfvénic and we enter into the MHD regime (see discussion in Lazarian 2006b). For the param-

eters above the scale  $l_A \sim 0.1 - 1$  kpc, but the actual number of  $M_A$  is not certain and therefore our estimate of  $l_A$  should be treated with caution. Fortunately, the above uncertainty does not change the results of our paper appreciably.

Compressible MHD turbulence is a subject where a number of important insights have been obtained much before these ideas can be tested; the pioneering works in the area include Montgomery & Turner (1981), Shebalin et al. (1983), Higdon (1984). The key idea of critical balance by Goldreich & Sridhar (1995) has influenced in a profound way our further thinking of the MHD cascade.

In the MHD regime, at smaller scales where  $V_l \leq v_A$ , three types of modes should exist in a compressible magnetized plasma: Alfvén, slow and fast modes. Slow and fast modes may be roughly thought as the MHD counterpart of the compressible modes, while Alfvén modes may be thought as the MHD counterpart of solenoidal Kolmogorov eddies (a more extended discussion can be found in Cho, Lazarian & Vishniac 2002, and ref. therein).

Turbulence in the IGM is most likely a complex mixture of several turbulent modes. We shall assume that a sizeable part of turbulence at large scales (namely at scales where the magnetic tension does not affect the turbulent motions) is in the form of compressible motions. This is reasonable as these modes are easily generated in high beta medium (eg. Brunetti & Lazarian 2007 and ref. therein). Situation may be radically different at smaller scales where the magnetic field tension affects turbulent motions, i.e. in the MHD- regime,  $l \leq l_A$ . In this case, MHD numerical simulations have shown that a solenoidal turbulent forcing gets the ratio between the amplitude of Alfvén and fast modes in the form (Cho & Lazarian 2003) :

$$\frac{(\delta V)_c^2}{(\delta V)_s^2} \sim \frac{(\delta V)_s v_A}{c_s^2 + v_A^2} \quad (1)$$

which essentially means that coupling between these two modes may be important only at  $l \approx l_A$  (in the MHD- regime it should be  $(\delta V)_s \leq v_A$ ) since the drain of energy from Alfvénic cascade is marginal when the amplitudes of perturbations become weaker. Most importantly in galaxy clusters it is  $c_s^2 \gg v_A^2$  and thus the ratio between the amplitude of Alfvén and fast modes at scales  $l < l_A$  is expected to be small,  $(\delta V)_c^2/(\delta V)_s^2 \leq (v_A/c_s)^2 \sim 10^{-2}$  (this for solenoidal forcing at  $l \approx l_A$ ).

A more recent work by Kowal & Lazarian (2010) decomposed turbulent motions into slow, fast and Alfvén modes using wavelets. This approach is better justified than the decomposition in Fourier space employed in Cho & Lazarian (2002, 2003). Indeed, Alfvén and slow modes are defined in the local system of coordinates (see Lazarian & Vishniac 1999, Cho & Vishniac 2000, Maron & Goldreich 2001) and therefore the procedure of Fourier decomposition by Cho & Lazarian (2002, 2003, see 2005 for a review) can only be statistically true. The wavelet decomposition procedure is more localized in space and therefore is potentially more precise. Nevertheless, the results on mode decomposition in Kowal & Lazarian (2010) agree well with those in Cho & Lazarian (2003), which provides us with more confidence about the properties of MHD turbulence that we employ in the paper to describe turbulence interaction with energetic particles.

Our treatment of turbulence assumes that the turbu-

lence is balanced, i.e. the energy flux of waves<sup>†</sup> moving in one direction is equal to the energy flux in the opposite direction. While the theory of imbalanced turbulence is being intensively developed (see Lithwick & Goldreich 2001; Beresnyak & Lazarian 2008, 2009, 2010; Chandran 2008, Perez & Boldyrev 2009) we do not expect that the effects of imbalance would dominate in the cluster environments. First of all, the turbulence driving is not expected to be strongly localized and then the effects of compressibility should decrease the local turbulence imbalance.

### 3 PARTICLE ACCELERATION, ENERGY LOSSES AND SECONDARY PARTICLES

In this paper we provide an extension of our previous calculations. We assume the picture of MHD turbulence in the IGM, as derived in Brunetti & Lazarian (2007), to calculate the reacceleration of relativistic particles by compressible MHD turbulence by taking into account self-consistently also the generation and reacceleration of secondary particles. The aim of this Section is to present the formalism and the main assumptions used in our calculations.

#### 3.1 Basic formalism

We model the re-acceleration of relativistic particles by MHD turbulence in the most simple situation in which only relativistic protons are initially present in a turbulent IGM. These protons generate secondary electrons via p-p collisions and in turns secondaries (as well as protons) are reaccelerated by MHD turbulence.

We model the time evolution of the spectral energy distribution of electrons,  $N_e^-$ , and positrons,  $N_e^+$ , with an isotropic Fokker-Planck equation<sup>‡</sup>:

$$\begin{aligned} \frac{\partial N_e^\pm(p, t)}{\partial t} = & \frac{\partial}{\partial p} \left[ N_e^\pm(p, t) \left( \left| \frac{dp}{dt} \right|_r - \frac{1}{p^2} \frac{\partial}{\partial p} (p^2 D_{pp}^\pm) \right. \right. \\ & \left. \left. + \left| \frac{dp}{dt} \right|_i \right) \right] + \frac{\partial^2}{\partial p^2} [D_{pp}^\pm N_e^\pm(p, t)] \\ & + Q_e^\pm[p, t; N_p(p, t)], \end{aligned} \quad (2)$$

where  $|dp/dt|$  marks radiative (r) and Coulomb (i) losses (Sect. 3.3),  $D_{pp}$  is the electron/positron diffusion coefficient in the momentum space due to the coupling with magnetosonic modes (Sect. 3.2), and the term  $Q_e^\pm$  accounts for the injection rate of secondary electrons and positrons due to p-p collisions in the IGM (Sect. 3.4).

The time evolution of the spectral energy distribution of protons,  $N_p$ , is given by:

$$\frac{\partial N_p(p, t)}{\partial t} = \frac{\partial}{\partial p} \left[ N_p(p, t) \left( \left| \frac{dp}{dt} \right| - \frac{1}{p^2} \frac{\partial}{\partial p} (p^2 D_{pp}) \right) \right]$$

<sup>†</sup> Strong MHD turbulence presents a case of dualism of waves and eddies (see Lazarian & Vishniac 1999; Cho, Lazarian & Vishniac 2003). Strong non-linear damping of oppositely moving Alfvénic wave packets makes them act like eddies.

<sup>‡</sup> isotropization of particles is discussed in Sect. 3.2.

$$+ \frac{\partial^2}{\partial p^2} [D_{pp} N_p(p, t)] - \frac{N_p(p, t)}{\tau_{pp}(p)}, \quad (3)$$

where  $|dp/dt|$  marks Coulomb losses (Sect. 3.3),  $D_{pp}$  is the diffusion coefficient in the momentum space of protons due to the coupling with magnetosonic modes (Sect. 3.2), and  $\tau_{pp}$  is the proton life-time due to pp collisions in the IGM (Sect. 3.3; see also Ensslin et al 2007).

For isotropic turbulence (Sect. 3.2) the diffusion equation in the k-space is given by:

$$\begin{aligned} \frac{\partial \mathcal{W}(k, t)}{\partial t} = & \frac{\partial}{\partial k} \left( k^2 D_{kk} \frac{\partial}{\partial k} \left( \frac{\mathcal{W}(k, t)}{k^2} \right) \right) + I(k, t) \\ & - \sum_i \Gamma_i(k, t) \mathcal{W}(k, t), \end{aligned} \quad (4)$$

where  $D_{kk}$  is the diffusion coefficient in the k-space,  $\Gamma_i(k, t)$  are the different damping terms, and  $I(k, t) = I_o \delta(k - k_o)$  is the turbulence injection term, i.e. we consider the most simple situation where turbulence is injected at a single scale, with wavenumber  $k_o$ . The wave-wave diffusion coefficient of magnetosonic modes (Kraichnan treatment) is given by (Brunetti & Lazarian 2007 and ref therein):

$$D_{kk} \approx \langle V_{ph} \rangle k^4 \left( \frac{\mathcal{W}(k, t)}{\rho \langle V_{ph} \rangle^2} \right) \quad (5)$$

where  $\langle V_{ph} \rangle$  is a representative, averaged (with respect to  $\theta$ ), phase velocity.

We shall assume isotropic MHD turbulence to calculate the particle acceleration rate at any time. This assumption is appropriate for super-Alfvénic turbulence and fast modes (e.g., Cho & Lazarian 2003), provided that collisionless dampings are not efficient. At smaller scales, collisionless dampings with thermal particles in the IGM become severe and modify the spectrum of turbulent modes, and a cut-off in the turbulent spectrum is generated at  $k = k_c$ , where the damping time-scale becomes shorter than the cascading time. The most important damping with thermal (and relativistic) particles is the Transit-Time-Damping (TTD) that is highly anisotropic (e.g. Schlickeiser & Miller 1998; Brunetti & Lazarian 2007; Yan et al. 2008) being stronger for  $\theta \sim \pi/2$  and causing the spectrum of the turbulent modes to become anisotropic at scales  $k \sim k_c(\theta)$ . On the other hand, in Brunetti & Lazarian (2007) we have shown that, under physical conditions typical of the IGM, hydro-motions bend the magnetic-field lines in a time-scale,  $\tau_{bb} \approx l_A/v_A$ , that is comparable to the damping time-scale of turbulence, in which case there is chance that approximate isotropization of the turbulent spectrum is maintained even at scales where dampings are severe.

Thus following Brunetti & Lazarian (2007) we shall assume a simplified turbulent (isotropic) spectrum in the form:

$$\mathcal{W}(k) \approx (I_o \rho \langle V_{ph} \rangle)^{\frac{1}{2}} k^{-\frac{3}{2}} \quad (6)$$

for  $k_o < k < k_c$ , with the cut-off wavenumber estimated from the condition that the damping time-scale becomes smaller than the cascading time scale:

$$\tau_d \approx 1 / \left\langle \sum_i \Gamma_i(k, \theta) \right\rangle = \tau_{kk} \approx k^2 / D_{kk} \quad (7)$$

that is:

$$k_c = C \frac{I_o}{\rho \langle V_{\text{ph}} \rangle} \left( \frac{\langle \sum \Gamma_i(k, \theta) \rangle}{k} \right)^{-2} \quad (8)$$

where quantities  $\langle \dots \rangle$  are averaged with respect to  $\theta$  and  $\sum \Gamma_i$  is the total (thermal and non-thermal) damping term due to TTD resonance and the constant  $C \sim$  a few (Brunetti & Lazarian 2007; see also Matthaeus & Zhou 1989, for details on Kraichnan constants).

### 3.2 Momentum diffusion coefficient due to compressible MHD turbulence

Compressible turbulence can affect particle motion through the action of the mode–electric field via gyroresonant interaction (e.g., Melrose 1968), the condition for which is :

$$\omega - k_{\parallel} v_{\parallel} - n \frac{\Omega}{\gamma} = 0 \quad (9)$$

where  $n = \pm 1, \pm 2, \dots$  gives the first (fundamental), second, .. harmonics of the resonance, while  $v_{\parallel} = \mu v$  and  $k_{\parallel} = \eta k$  are the parallel (projected along the magnetic field) speed of the particles and the wave–number, respectively.

Following Brunetti & Lazarian (2007) we assume particle–mode coupling through the Transit–Time Damping (TTD),  $n = 0$ , resonance (e.g., Fisk 1976; Eilek 1979; Miller, Larosa & Moore 1996; Schlickeiser & Miller 1998). In principle, this resonance changes only the component of the particle momentum parallel to the seed magnetic field and this would cause an increasing degree of anisotropy of the particle distribution leading to a less and less efficient process with time. Thus an important aspect in this working picture is the need of isotropization of particle momenta during acceleration (e.g., Schlickeiser & Miller 1998). In this paper we shall assume continuous isotropization of particle momenta. Isotropy may be provided by several processes discussed in the literature. These include electron firehose instability (Pilipp & Völk 1971; Paesold & Benz 1999), and gyro–resonance by Alfvén (and slow) modes at small scales, provided that these modes are not too much anisotropic (cf. Yan & Lazarian 2004)<sup>§</sup>. Gyro–resonance may also occur with electrostatic lower hybrid modes generated by anomalous Doppler resonance instability due to pitch angle anisotropies (e.g., Liu & Mok 1977; Moghaddam–Taaheri et al. 1985) and, possibly, with whistlers (e.g., Steinacker & Miller 1992). In addition, Lazarian & Beresnyak (2006) proposed isotropization of cosmic rays due to *gyroresonance instability* that arises as the distribution of cosmic rays gets anisotropic in phase space.

We adopt the momentum–diffusion coefficient of particles,  $D_{pp}$ , as derived from detailed balancing argument, i.e. relating the diffusion coefficient of a  $\alpha$ –species to the damping rate of the modes themselves with the same particles (e.g., Eilek 1979; Brunetti & Lazarian 2007)<sup>¶</sup> :

<sup>§</sup> The latter condition means that the Alfvénic modes are considered for scales not much less than  $l_A$ , provided that the turbulence injection is isotropic

<sup>¶</sup> This is obtained by assuming that particles isotropy is *maintained* during acceleration (see Brunetti & Lazarian 2007)

$$D_{pp}(p) = \frac{\pi^2}{2c} p^2 \frac{1}{B_o^2} \int_0^{\pi/2} d\theta V_{\text{ph}}^2 \frac{\sin^3(\theta)}{|\cos(\theta)|} \mathcal{H} \left( 1 - \frac{V_{\text{ph}}/c}{\cos \theta} \right) \times \left( 1 - \left( \frac{V_{\text{ph}}/c}{\cos \theta} \right)^2 \right)^2 \int_{k_c} dk \mathcal{W}_B(k) k \quad (10)$$

where  $B_o$  is the background (unperturbed) magnetic field,  $k_c$  is given in Eq. 8 and

$$\mathcal{W}_B(k) = \frac{1}{\beta_{pl}} \left\langle \frac{\beta_{pl} |B_k|^2}{16\pi \mathcal{W}(k)} \right\rangle \mathcal{W}(k) \quad , \quad (11)$$

where  $|B_k|^2/\mathcal{W}(k)$  is the ratio between magnetic field fluctuations and total energy in the mode (the quantity  $\langle \dots \rangle$  in Eq. 11 indicates average with respect to  $\theta$  and is of order unity, see Brunetti & Lazarian 2007 for further details).

### 3.3 Energy losses for electrons and protons

The energy losses of relativistic electrons in the IGM are dominated by ionization and Coulomb losses, at low energies, and by synchrotron and IC losses, at higher energies (eg. Sarazin 1999). The rate of losses due to the combination of ionization and Coulomb scattering is (in cgs units):

$$\left( \frac{dp}{dt} \right)_i = -3.3 \times 10^{-29} n_{\text{th}} \left[ 1 + \frac{\ln(\gamma/n_{\text{th}})}{75} \right] \quad (12)$$

where  $n_{\text{th}}$  is the number density of the thermal plasma. The rate of synchrotron and IC losses is (in cgs units):

$$\left( \frac{dp}{dt} \right)_{\text{rad}} = -4.8 \times 10^{-4} p^2 \left[ \left( \frac{B_{\mu G}}{3.2} \right)^2 \frac{\sin^2 \theta}{2/3} + (1+z)^4 \right] \quad (13)$$

where  $B_{\mu G}$  is the magnetic field strength in units of  $\mu G$ , and  $\theta$  is the pitch angle of the emitting leptons; in case of efficient isotropization of the electron momenta, the  $\sin^2 \theta$  is averaged to 2/3.

For relativistic protons, the main channel of energy losses in the IGM is provided by inelastic p-p collisions. The life–time of protons due to pp collisions is given by :

$$\tau_{pp}(p) = \frac{1}{c n_{\text{th}} \sum \sigma^{+/-,o}} \quad (14)$$

In this paper we use the inclusive cross section,  $\sigma^{\pm,o}(pp)$ , given by the fitting formulae in Dermer (1986a) which allow to describe separately the rates of generation of neutral and charged pions.

For trans-relativistic and mildly relativistic protons, energy losses are dominated by ionization and Coulomb scattering. Protons more energetics than the thermal electrons, namely with  $\beta_p > \beta_c \equiv (3/2 m_e/m_p)^{1/2} \beta_e$  ( $\beta_e \simeq 0.18(T/10^8 K)^{1/2}$  is the velocity of the thermal electrons), are affected by Coulomb interactions. Defining  $x_m \equiv \left( \frac{3\sqrt{\pi}}{4} \right)^{1/3} \beta_e$ , one has (Schlickeiser, 2002):

$$\left( \frac{dp}{dt} \right)_i \simeq -1.7 \times 10^{-29} \left( \frac{n_{\text{th}}}{10^{-3}} \right) \frac{\beta_p}{x_m^3 + \beta_p^3} \quad (\text{cgs}) \quad (15)$$

### 3.4 Injection of Secondary Electrons

The decay chain that we consider for the injection of secondary particles in the IGM due to p-p collisions is (Blasi & Colafrancesco 1999):

$$p + p \rightarrow \pi^0 + \pi^+ + \pi^- + \text{anything}$$

$$\pi^0 \rightarrow \gamma\gamma$$

$$\pi^\pm \rightarrow \mu + \nu_\mu \quad \mu^\pm \rightarrow e^\pm \nu_\mu \nu_e.$$

that is a threshold reaction that requires protons with kinetic energy larger than  $T_p \approx 300$  MeV.

A practical and useful approach to describe the pion spectrum both in the high energy ( $E_p > 10$  GeV) and low energy regimes was proposed in Dermer (1986b) and reviewed by Moskalenko & Strong (1998) and Brunetti & Blasi (2005), and is based on the combination of the isobaric model (Stecker 1970) and scaling model (Badhwar et al., 1977; Stephens & Badhwar 1981).

The injection rate of pions is given by :

$$Q_\pi^{\pm,0}(E, t) = n_{th}^p c \int_{p_{tr}} dp N_p(p, t) \beta_p \frac{F_\pi(E_\pi, E_p) \sigma^{\pm,0}(p_p)}{\sqrt{1 + (m_p c/p_p)^2}}, \quad (16)$$

where we adopted  $F_\pi$  as given in Brunetti & Blasi (2005) that use the isobaric model for  $E_p < 3$  GeV, a scaling model for  $E_p > 10$  GeV and a linear combination of the two models for intermediate energies, and where  $p_{tr}$  is the threshold momentum of protons for the process to occur.

The injection rate of relativistic electrons/positrons is given by :

$$Q_{e^\pm}(p, t) = \int_{E_\pi} Q_\pi(E_{\pi^\pm}, t) dE_\pi \int dE_\mu \times F_{e^\pm}(E_\pi, E_\mu, E_e) F_\mu(E_\mu, E_\pi), \quad (17)$$

where  $F_e^\pm(E_e, E_\mu, E_\pi)$  is the spectrum of electrons and positrons from the decay of a muon of energy  $E_\mu$  produced in the decay of a pion with energy  $E_\pi$ , and  $F_\mu(E_\mu, E_\pi)$  is the muon spectrum generated by the decay of a pion of energy  $E_\pi$  that is :

$$F_\mu(E_\mu, E_\pi) = \frac{m_\pi^2}{m_\pi^2 - m_\mu^2} \frac{1}{\sqrt{E_\pi^2 - m_\pi^2}} \quad (18)$$

between a kinematic minimum and maximum muon energy given by :

$$m_\mu \gamma_\pi \gamma'_\mu (1 - \beta_\pi \beta'_\mu) \leq E_\mu \leq m_\mu \gamma_\pi \gamma'_\mu (1 + \beta_\pi \beta'_\mu) \quad (19)$$

where  $\gamma'_\mu$  is the Lorentz factor of the muon in the pion frame,  $\beta'_\mu \simeq 0.2714$  (Moskalenko & Strong 1998), and from kinematics :

$$m_\mu \gamma'_\mu \beta'_\mu = \frac{m_\pi^2 - m_\mu^2}{2m_\pi}. \quad (20)$$

In order to simplify calculations, following Brunetti & Blasi (2005), we assume that the spectrum of muons is a delta-function :

$$F_\mu(E_\mu, E_\pi) = \delta(E_\mu - \bar{E}_\mu), \quad (21)$$

where

$$\bar{E}_\mu = \frac{m_\pi^2 - m_\mu^2}{m_\pi^2} \frac{E_\pi}{2\beta'_\mu}. \quad (22)$$

We use the spectrum of electrons and positrons from the muon decay,  $F_{e^\pm}(E_\pi, E_\mu, E_e)$ , as given by Blasi & Colafrancesco (1999), and combining their results with Eqs.

(16), (17) and (21), we obtain the rate of production of secondary electrons/positrons :

$$Q_{e^\pm}(p, t) = \frac{8\beta'_\mu m_\pi^2 n_{th}^p c}{m_\pi^2 - m_\mu^2} \int_{E_{\min}} \int_{E_*} \frac{dE_\pi dE_p}{E_\pi \beta'_\mu} \beta_p N(E_p) \times \sqrt{1 - \left(\frac{m_p c^2}{E_p}\right)^2} \sigma^\pm(E_p) F_\pi(E_\pi, E_p) \tilde{F}, \quad (23)$$

where  $E_{\min} = 2E_e \beta'_\mu m_\pi^2 / (m_\pi^2 - m_\mu^2)$ , and

$$\tilde{F} = \frac{5}{12} - \frac{3}{4} \bar{\lambda}^2 + \frac{1}{3} \bar{\lambda}^3 - \frac{\bar{P}_\mu}{2\bar{\beta}_\mu} \left( \frac{1}{6} - (\bar{\beta}_\mu + \frac{1}{2}) \bar{\lambda}^2 + (\bar{\beta}_\mu + \frac{1}{3}) \bar{\lambda}^3 \right),$$

$$\text{for } \frac{1 - \bar{\beta}_\mu}{1 + \bar{\beta}_\mu} \leq \bar{\lambda} \leq 1;$$

and

$$= \frac{\bar{\lambda}^2 \bar{\beta}_\mu}{(1 - \bar{\beta}_\mu)^2} \left[ 3 - \frac{2}{3} \bar{\lambda} \left( \frac{3 + \bar{\beta}_\mu^2}{1 - \bar{\beta}_\mu} \right) \right] - \frac{\bar{P}_\mu}{1 - \bar{\beta}_\mu} \left\{ \bar{\lambda}^2 (1 + \bar{\beta}_\mu) - \frac{2\bar{\lambda}^2}{1 - \bar{\beta}_\mu} \left[ \frac{1}{2} + \bar{\lambda} (1 + \bar{\beta}_\mu) \right] + \frac{2\bar{\lambda}^3 (3 + \bar{\beta}_\mu^2)}{3(1 - \bar{\beta}_\mu)^2} \right\},$$

$$\text{for } 0 \leq \bar{\lambda} \leq \frac{1 - \bar{\beta}_\mu}{1 + \bar{\beta}_\mu}.$$

and where we use the following definitions :

$$\bar{\lambda} = \frac{E_e}{E_\pi} = \frac{E_e}{E_\pi} \left( \frac{2\beta'_\mu m_\pi^2}{m_\pi^2 - m_\mu^2} \right), \quad (24)$$

$$\bar{\beta}_\mu = \left( 1 - \frac{m_\mu^2}{E_\mu^2} \right)^{1/2} \quad (25)$$

and

$$\bar{P}_\mu = -\frac{1}{\bar{\beta}_\mu} \frac{m_\pi^4}{(m_\pi^2 - m_\mu^2)^2} \left[ 4\beta'_\mu - 1 + \left( \frac{m_\mu}{m_\pi} \right)^4 \right]. \quad (26)$$

## 4 RESULTS

In this Section we calculate particle acceleration and non-thermal emission in galaxy clusters by assuming that MHD turbulence is generated during mergers between clusters and reaccelerates primary and secondary particles.

Following previous works (eg. Brunetti & Blasi 2005) we adopt a simplified situation where we do not consider primary electrons in the IGM (see Sect.5 for discussion), and where the two main ingredients are (i) relativistic protons, that are believed to be the most important non-thermal particle components in the IGM (eg., Blasi et al 2007 for review), and (ii) the MHD turbulence. On one hand, relativistic protons inject secondary particles via p-p collisions in the IGM that produce radiation from the radio to the gamma ray band, at the same time MHD turbulence may reaccelerate relativistic protons and secondary electrons in the IGM, generating radio halos and leaving an imprint in the general non-thermal properties of galaxy clusters.

At variance with the aforementioned paper that focus on the Alfvénic case, following the model of MHD turbulence in galaxy clusters by Brunetti & Lazarian (2007), we

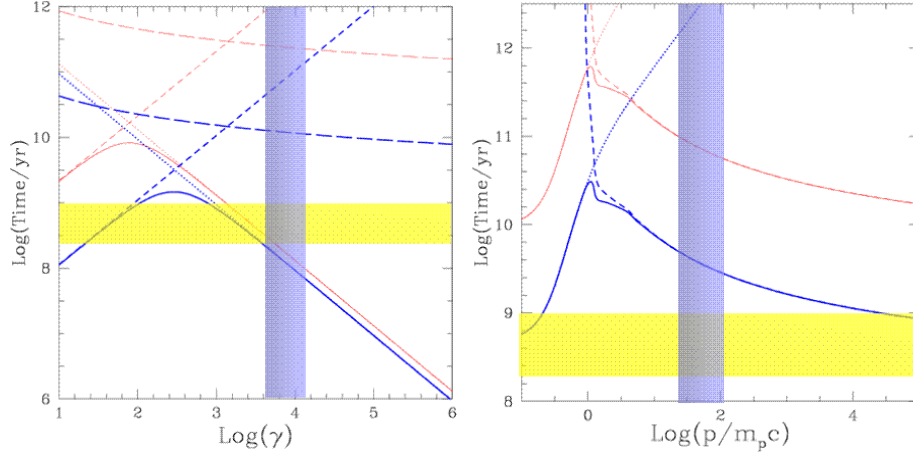


**Figure 1.** **Left panel:** The life–time of relativistic electrons in the IGM at  $z = 0.2$  as a function of their Lorentz factor. Thick (blue) lines are for cluster cores ( $B = 3\mu\text{G}$ ,  $n_{th} = 2 \times 10^{-3}\text{cm}^{-3}$ ) and thin (red) lines are for cluster periphery ( $B = 0.5\mu\text{G}$ ,  $n_{th} = 10^{-4}\text{cm}^{-3}$ ). We report the total life–time (solid lines) and the life–times due to single processes: Coulomb losses (dashed lines), synchrotron and IC losses (dotted lines), and bremsstrahlung losses (long dashed lines). The yellow region marks the turbulence eddy turnover time (assuming  $L_o \sim 200 - 300$  kpc,  $(V_L/c_s)^2 \approx 0.1 - 0.3$ ,  $T \approx 10^8$  K), while the blue region marks the range of Lorentz factors of the relativistic electrons emitting at frequencies  $\approx 300 - 1400$  MHz. **Right panel:** The life–time of cosmic–ray protons in the IGM as a function of the particle momentum. Thick (blue) lines are for cluster cores and thin (red) lines are for cluster periphery. We report the total life–time (solid lines) and the life–times due to single processes: Coulomb losses (dotted lines) and pp–collisions (dashed lines). The yellow region marks the turbulence eddy turnover time, while the blue region marks the range of momentum of relativistic protons that mostly contribute to the injection of secondary electrons emitting at frequencies  $\approx 300 - 1400$  MHz.

assume that MHD turbulence in the IGM is in the form of compressible modes whose cascading from large to small scales results in a isotropic turbulent–spectrum. This allows us to readily connect the injection of turbulence at large scales with the particle acceleration process and to study the theoretical framework of the connection between cluster mergers and turbulent reacceleration of relativistic particles in the IGM. As a matter of fact calculations reported in this Section provide an extension of those in Brunetti & Lazarian (2007) that consider reacceleration of (only) primary particles by compressible MHD modes.

As already stressed, one of the main motivations for these new calculations comes from the recent gamma ray and radio observations that put severe constraints on the energy density of relativistic protons in galaxy clusters (Brunetti et al 2007; Aharonian et al 2009a,b; Aleksic et al 2010; Ackermann et al 2010), allowing for including secondary particles in turbulent–acceleration models with substantially less degree of freedom than in the past.

#### 4.1 Turbulent reacceleration, time–scales and connection with mergers

In the framework adopted in our paper the idea is that radio halos are generated by the reacceleration of relativistic electrons (secondaries in our specific case) by turbulence generated during cluster mergers.

The leading processes in the context of our scenario are the generation, cascading and dissipation of turbulence in the IGM, and the acceleration and cooling of relativistic particles. These processes, and the cluster–cluster collisions themselves, have their own time–scale and the general picture breaks out from the interplay of all these time–scales. Fig-

ure 1 reports the time–scales of the most relevant processes as calculated in different, relevant, regions of the cluster volume.

The generation and dissipation of turbulent motions in the IGM is not studied in great details, however present numerical simulations suggest that these motions can be generated in galaxy clusters for a substantial fraction of the period of cluster–cluster interaction, a few Gyr, possibly driven by shock waves that cross the cluster volume and by the sloshing (and stripping) of cluster cores (e.g., Dolag et al. 2005; Vazza et al. 2009a; Paul et al. 2010; ZuHone et al. 2010). Under our working picture, the compressible turbulence, after being injected at larger scales, decays at smaller scales where it dissipates through dampings with thermal and non–thermal particles in the IGM (Sect. 3.1). The turbulence decay requires about one eddy turnover time, that in the case of fast mode is  $\tau_{kk} \sim \frac{V_{ph}}{V_L^2} (L/k)^{1/2}$  (e.g., Yan & Lazarian 2004), implying a unavoidable delay between the first generation of large–scale turbulence in a given region and the beginning of the phase of particle reacceleration (that is mainly due to the non linear interaction of particles with turbulent modes at smaller scales) in the same region. We believe however that this delay does not break the temporal connection between mergers and particle acceleration, since the eddy turnover time of compressible turbulence in massive (hot) clusters is  $\tau_{kk} \approx 0.2 - 1$  Gyr (by assuming typical injection scales  $L_o \approx 200 - 300$  kpc and  $(V_L/c_s)^2 \approx 0.1 - 0.3$ ), that is smaller than the typical duration of cluster–cluster interaction.

Under our simplified working picture, where turbulence is (only) generated by energetic cluster mergers, compressible turbulence dissipates completely in a few eddy turnover times, as soon as galaxy clusters becomes more relaxed. The



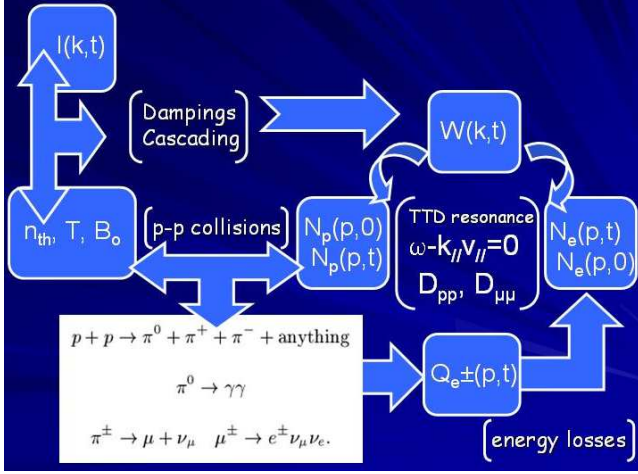


**Figure 2.** A scheme of the processes taken into account in our calculations and the coupling between them. The starting points are the properties of the magnetized IGM ( $n_{th}, T, B_0$ ), the initial spectrum of relativistic protons ( $N_p(p, 0)$ ) and the injection rate of turbulence ( $I(k)$ ).

decrease of the efficiency of turbulent–particle acceleration and the suppression of non-thermal cluster–scale emission, i.e. the “dissipation” of radio halos, are even faster due to the fact that (i) the acceleration efficiency scales non linearly with the turbulent spectrum<sup>||</sup> and (ii) the cooling time of the radio–emitting electrons is short,  $\approx 0.1$  Gyr (Fig. 1). The consequence is a tight connection between radio halos and cluster mergers, although the picture may be more complex as the secondary particles, continuously injected in the IGM, should generate synchrotron emission at some level also in relaxed clusters (see Sect. 4.3.2).

Radio observations of statistical samples of galaxy clusters show that (i) giant radio halos form (only) in merging clusters, (ii) that their life–time in merging clusters is of the order of 1 Gyr, and (iii) suggest that halo emission should dissipate in relaxed clusters in a short,  $< 1$  Gyr, time-scale (e.g. Hwang 2004; Brunetti et al. 2007, 2009b; Venturi et al 2008); these observational points are consistent with the working picture described in this Section.

## 4.2 Spectral evolution of reaccelerated protons and electrons

In this Section we report on some relevant results on the evolution of the particles spectrum (protons and secondary electrons/positrons) subject to TTD resonance with compressible MHD turbulence; the approach followed in this section is than used in next Section to calculate non–thermal emission from galaxy clusters.

We adopt a simplified situation: Figure 2 shows the chain of physical processes that we consider and their interplay. We assume that the thermal IGM is magnetized and, at time = 0, consider (only) relativistic protons, with initial spectrum  $N_p(p) = K_p p^{-2.6}$ . The presence of relativistic and thermal protons determines the initial efficiency of injection

of secondary particles in the IGM (Sect. 3.4), whose initial spectrum is calculated assuming stationary conditions (e.g. Dolag & Ensslin 2000; i.e. by taking  $D_{pp} = 0$  and  $\partial N/\partial t = 0$  in Eq. 2).

Following Brunetti & Lazarian (2007), we assume that compressible turbulence is injected at large scales and develops a quasi–stationary spectrum (Eq. 6) due to the interplay between non-linear wave-wave interaction and collisionless dampings at smaller scales (Sect. 3.1). Following Brunetti & Lazarian (2007) we consider a time–independent damping,  $\sum \Gamma_i \simeq \Gamma_{th}$ , that is obtained by assuming the (initial) physical properties of the IGM. This is motivated by the fact that in our model TTD dampings with relativistic particles are sub-dominant with respect to those with thermal IGM (see Cassano & Brunetti 2005 and Brunetti & Lazarian 2007) and by the fact that the thermal properties of the IGM are not greatly modified by turbulence.

In our calculations we follow self-consistently the re-acceleration of relativistic protons due to TTD with the compressible turbulent-modes, the generation (and its evolution with time due to the evolution of the spectrum of protons) of secondary electrons and positrons through collisions between these protons and the IGM, and the reacceleration of the secondaries (see Fig. 2).

Theoretically we expect that magnetic field can be amplified by turbulence in the IGM (e.g. Subramanian et al 2006), although as a necessary simplification we do not include that amplification process in our calculations. The main reason is that the spectrum of the reaccelerated relativistic electrons is expected to evolve more rapidly than the magnetic field in the IGM (e.g. Cassano 2010). We also stress that present data do not show a clear connection between the magnetic field properties and cluster dynamics (e.g. Clarke et al 2001; Govoni 2006) that leaves the process of magnetic field amplification still poorly constrained.

Turbulent acceleration can be thought as the combination of a systematic effect, that causes the boosting of the spectrum of particles at higher energies, and a stochastic effect, that causes a broadening of the spectrum with no net acceleration (e.g. Melrose 1968; Petrosian 2001). The time-scale of the systematic acceleration is :

$$\tau_{acc} = \frac{p^3}{\partial p^2 D_{pp} / \partial p} = \frac{p^2}{4D_{pp}} \quad (27)$$

that does not depend on the particle energy in the case of TTD acceleration (Sect. 3.2), provided that the spectrum of compressible turbulence is isotropic (Sect. 3.1).

By considering a reference value of the acceleration time due to TTD resonance in the IGM,  $\tau_{acc} \approx 10^8$  yrs (e.g., Cassano & Brunetti 2005; Brunetti & Lazarian 2007), Coulomb\*\* and radiative losses in the IGM prevent the reacceleration of electrons with energies  $E < 10$  MeV and  $E > 10$  GeV, respectively (Fig.1).

On the other hand, TTD resonance in the IGM may reaccelerate supra-thermal protons up to high energies, and consequently in our model the energy density of relativistic protons increases with mergers, similarly to the energy of the thermal IGM. By considering a toy scenario where these

<sup>||</sup> e.g.,  $\tau_{acc} \propto D_{pp} \propto W_k^2$ , combining Eqs. 6, 8 and 10, see also Brunetti & Lazarian (2007)

\*\* In the external regions of galaxy clusters Coulomb losses are less severe and lower energy electrons can be reaccelerated (Fig.1)



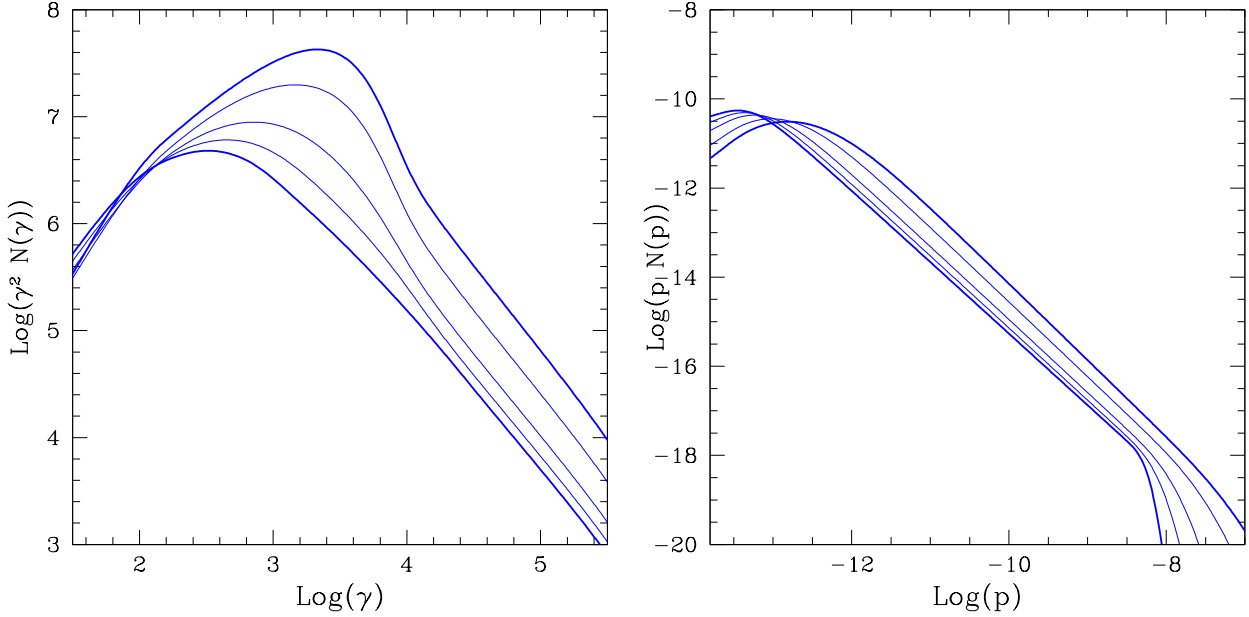


**Figure 3.** The time evolution of the spectrum of electrons (left panel) and protons (right panel). From bottom to top, calculations are shown after 0.3, 1, 2, 4,  $6.5 \times 10^8$  yrs of reacceleration. Calculations are obtained at  $z = 0$ , assuming  $(V_L/c_s)^2 = 0.22$ , with injection scale  $L_o = 300$  kpc,  $T = 10^8$  K, thermal density  $n_{th} = 2.64 \times 10^{-3} \text{cm}^{-3}$  and  $B = 4.69 \mu\text{G}$ .

protons are simply injected in the cluster volume, with initial energy density  $\epsilon_{CR}(0)$ , and then reaccelerated by MHD turbulence during major cluster mergers, the rate of increase of their energy is :

$$d\epsilon_{CR}/dt \sim \int dk W(k, t) \Gamma_{CR}(k, t) \quad (28)$$

where the TTD damping of compressible MHD turbulence by relativistic protons in case  $\beta_{pl} \gg 1$  (from Eq. 31 in Brunetti & Lazarian 2007) is :

$$\Gamma_{CR}/\omega_r \simeq \frac{\pi^2}{4} \frac{c_s}{c} \frac{\epsilon_{CR}}{\epsilon_{th}} \frac{\sin^2 \theta}{|\cos \theta|} \left\{ \frac{\partial \hat{f}}{\partial p} \right\} \quad (29)$$

where  $\{\dots\} = s+2$  assuming a power law energy distribution of relativistic protons  $N(p) \propto p^{-s}$ . By assuming a "sonic" turbulent-forcing,  $I_o \tau_{cl} \approx \epsilon_{th}$ , where  $\tau_{cl} \sim 3 - 6$  Gyrs is the life-time of massive clusters, and a typical merging history of massive clusters (eg., Cassano & Brunetti 2005 and ref. therein), we expect  $\epsilon_{CR} \leq$  few percent of the thermal energy density, provided that relativistic protons are injected in the IGM with an "initial" energy density  $\epsilon_{CR}(0)/\epsilon_{th} \sim 0.001 - 0.01^{\dagger\dagger}$ .

In Figure 3 we report the time evolution of relativistic electrons and protons in a hot,  $T \sim 10^8$  K, IGM by assuming  $(V_L/c_s)^2 = 0.22$ , in which case the TTD acceleration time is  $\tau_{acc} \sim 10^8$  yrs. Radiative losses prevent the acceleration of relativistic electrons above a maximum energy,  $\gamma_{max} \approx 10^4$ , producing a bump in the spectrum of electrons (Fig. 3a). The number density of high energy electrons increases with

time also for  $\gamma > \gamma_{max}$  (Fig. 3a), that is because the injection rate of secondary electrons is enhanced with time as protons are accelerated (Fig. 3b). Overall the mechanism is very efficient : on one hand the acceleration of relativistic protons enhances the injection rate of secondary electrons, at the same time an increasing number of secondary electrons accumulates at energies  $\approx \gamma_{max}$  where cooling is balanced by acceleration. The combination of these two effects boosts the spectrum of electrons at energies  $\gamma \approx \gamma_{max}$ .

In Figure 4 we report the evolution of the spectrum of electrons with time assuming physical conditions that span the volume occupied by radio halos, from cluster core (solid lines) to 1 Mpc distance from the cluster center (dashed lines);  $(V_L/c_s)^2 = 0.22$  is assumed in both cases. Figure 4 highlights the effect of decreasing radiative and Coulomb losses on the spectrum of the reaccelerated electrons : the boosting of the particle spectrum increases in the external (Mpc-distance) regions because Coulomb losses are less severe (which allows the reacceleration of the bulk of secondary electrons) and because synchrotron losses become sub-dominant with respect to inverse Compton losses due to the scattering of the CMB photons.

### 4.3 The non-thermal spectrum of turbulent galaxy clusters

In this Section we calculate the non thermal spectrum from galaxy clusters assuming reacceleration of primary protons and of their secondary products by compressible MHD turbulence in the IGM.

$\dagger\dagger$  this is obtained by using the approximate scalings  $\frac{kW(k)}{\tau_{kk}} \approx I_o$  in Eq.28

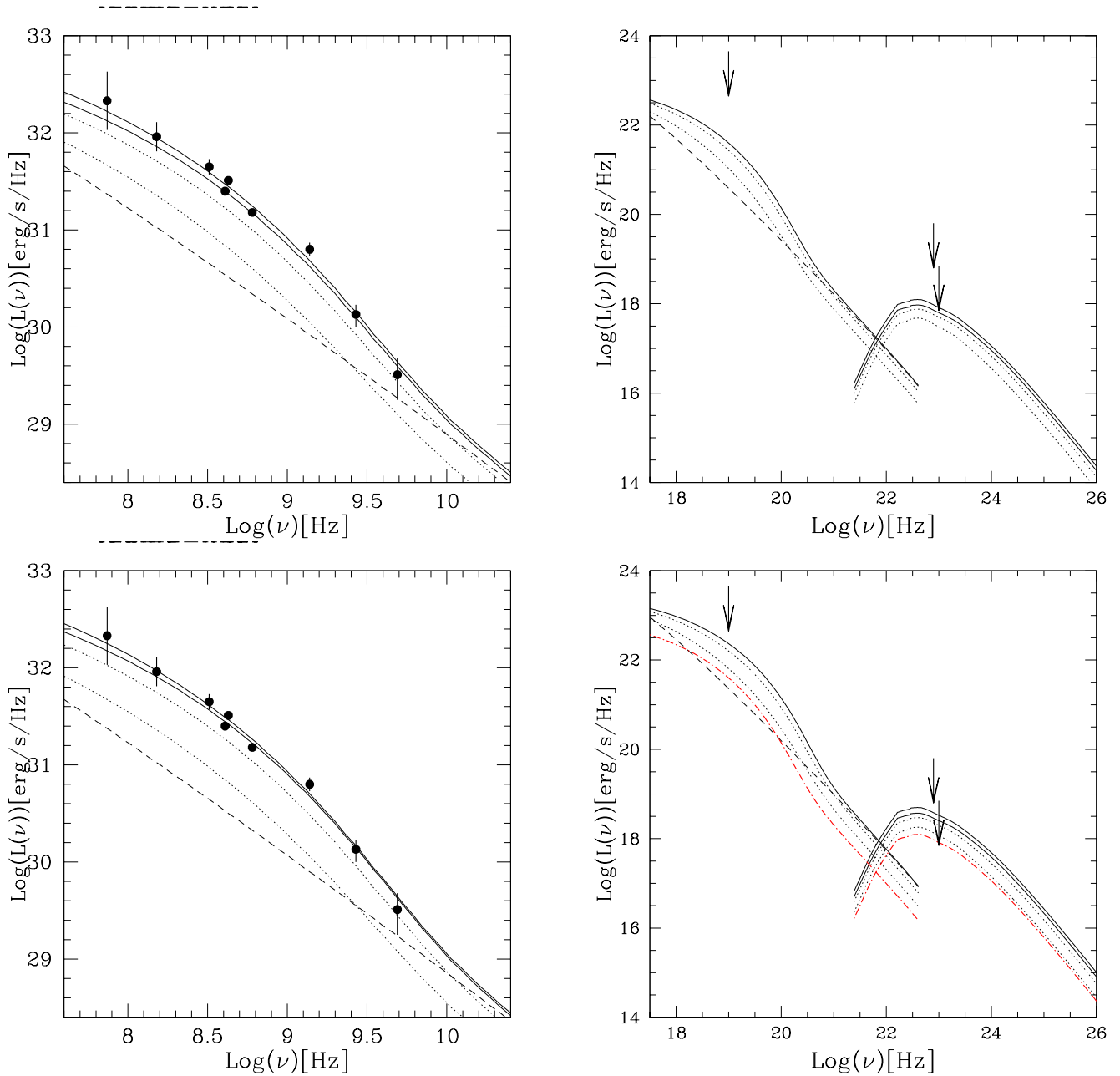


**Figure 5.** The radio (left) and high energy (right) emitted spectra from the Coma cluster (note that the SZ decrement at higher radio frequencies is not included, see e.g. Donnert et al. 2010b). **Upper panels** show our reference model (see text), **lower panels** refer to the case of a cluster magnetic field 2.5 times smaller than that in our reference model (for a better comparison red dot-dashed lines in the right panel show the IC and gamma-ray emission expected in our reference model). Solid lines show the emitted spectra obtained after  $6.5 \times 10^8$  yrs of reacceleration (upper and lower lines in the synchrotron and gamma-ray spectra refer to the emission within 4.5 and 3 core radii, respectively, while X-rays are calculated within 4.5 core radii), dashed lines show the emitted spectra obtained by assuming that MHD turbulence is dissipated in the cluster. Dotted lines show the emitted spectra at intermediate stages of reacceleration : after  $2$  and  $4 \times 10^8$  yrs, from bottom to top respectively. Radio data-points are taken from Thierbach et al (2003), the hard X-ray upper limit is from Suzaku observations (Wik et al 2008) and the EGRET and FERMI upper-limits are taken from Reimer et al (2003) and Ackermann et al (2010), respectively. Calculations assume  $(V_L/c_s)^2 \sim 0.18$  for our reference model and  $0.2$  for the lower panels ( $L_o = 300$  kpc is assumed in all calculations). For reference, the energy of the population of relativistic protons "measured" after 0.65 Gyr of reacceleration (solid lines) is 0.035 and 0.25 times that of the thermal cluster in our reference model and lower panels, respectively.

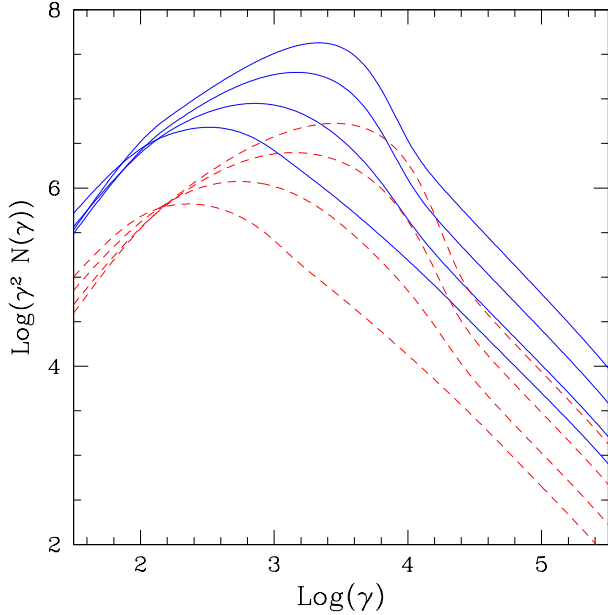


**Figure 4.** The time evolution of the spectrum of electrons in two different environments: in the clusters central regions (solid lines), assuming  $n_{th} = 2.64 \times 10^{-3} \text{cm}^{-3}$  and  $B = 4.69 \mu\text{G}$ , and in the clusters external regions (red dashed lines), assuming  $n_{th} = 0.56 \times 10^{-3} \text{cm}^{-3}$  and  $B = 2.16 \mu\text{G}$ . From bottom to top, calculations are shown after  $0.3, 2, 4$  and  $6.5 \times 10^8$  yrs of reacceleration. Calculations are obtained at  $z = 0$ , assuming  $(V_L/c_s)^2 = 0.22$ , with injection scale  $L_o = 300$  kpc,  $T = 10^8$  K.

#### 4.3.1 A toy model for the Coma cluster

The Coma cluster hosts the best studied, prototype, giant radio halo (Willson 1970; Giovannini et al 1993). Constraints on the high energy emission from the Coma cluster are presently available from hard X-ray (BeppoSAX, Fusco-Femiano et al 1999, 2004, Rossetti & Molendi 2004; RXTE, Rephaeli et al 1999; INTEGRAL, Eckert et al 2007, Lutovinov et al 2008; Suzaku, Wik et al 2009; Swift-BAT, Ajello et al 2009) and gamma ray (EGRET, Reimer et al 2003; FERMI, Ackermann et al 2010; HESS, Aharonian et al 2009b; VERITAS, Perkins 2008) observations. It is thus a natural first step to compare our model expectations with the spectral energy distribution (SED) of the non thermal emission from the Coma cluster.

We assume a simplified model for the thermal gas distribution in the Coma cluster that is anchored to the observed beta-model profile (e.g. Briel et al 1992, considering  $\Lambda\text{CDM}$  cosmology). The gas temperature,  $k_B T \simeq 8$  keV (David et al 1993), is assumed to be constant on Mpc-scale.

The magnetic field in the Coma cluster, and its spatial distribution, is a crucial ingredient in our modeling of the synchrotron (radio halo) properties. We adopt the recent results by Bonafede et al (2010) that carried out a detailed analysis of the Rotation Measures of a sample of extended cluster radio galaxies in the Coma cluster. The best fit to their data implies a magnetic field  $B(r) \propto \sqrt{n_{th}}$  with a central value  $B(0) \simeq 5 \mu\text{G}$ .

Once the thermal gas and magnetic field properties are anchored to present data, the free parameters in our calculations are (i) the energy density (and spatial distribution)

of relativistic protons (at time = 0)<sup>‡‡</sup>, and (ii) the injection rate (and scale) of compressible turbulence in the IGM,  $I_o$ . In our reference toy model we assume (i) a flat spatial distribution of relativistic protons on the halo-scale,  $r \sim 3 r_c$ , and a constant ratio between relativistic and thermal particles energy densities at larger distances, and (ii) a specific injection rate of turbulence,  $I_o/\rho$ , constant on the halo-scale. Assumption (i) is motivated by the fact that, similarly to other giant halos, the Coma radio halo has a very broad synchrotron-brightness distribution (Govoni et al 2001; see also discussion in Cassano et al 2007 and Donnert et al 2010a) implying a very broad spatial distribution of relativistic protons on the halo-scale. Assumption (ii) is motivated by hydrodynamical and MHD cosmological simulations that found very extended turbulent regions in simulated galaxy clusters (Sunyaev et al 2003; Dolag et al. 2005; Vazza et al 2009a; Paul et al 2010).

In Figure 5 (upper panels) we show the expected SED emitted by the Coma cluster (from  $r \leq 3 - 4.5 r_c$ ) assuming our reference model (see caption). We find that the radio spectrum of the Coma radio halo can be well reproduced by assuming a total energy content of relativistic protons, on the halo-scale,  $E_{CR} \sim 3.5\%$  of the thermal gas (see caption for details). The presence of a break in the spectrum of the Coma radio halo at higher frequencies has been interpreted as a signature of turbulent acceleration<sup>§§</sup>, since it implies a corresponding break in the spectrum of the emitting electrons at the energy where turbulent acceleration is balanced by radiative losses (e.g. Schlickeiser et al 1987; Brunetti et al 2001; Petrosian 2001). Figure 5 demonstrates that also models considering the reacceleration of secondary particles can explain the steepening of the Coma radio halo, although a tail at higher frequencies due to freshly-injected secondary electrons shows up in the (emitted) spectrum<sup>¶¶</sup>. For a consistency check, in Figure 6 we also show that, although very simplified, our reference model allows us to (roughly) reproduce the observed radio brightness profile of the Coma halo (although the predicted profile is still slightly steeper than the observed one). Such expected-broad synchrotron profile is due to the combination of the flat spatial distribution of relativistic protons with the increasing efficiency of reacceleration of secondary electrons at larger distances from the cluster centre (see Fig. 4).

The gamma ray emission from the cluster (from  $r \leq 3 - 4.5 r_c$ , see caption) is dominated by the decay process of  $\pi^0$  (Fig. 5) and is expected at about 10 percent level of the present gamma-ray upper limits (FERMI, Ackermann et al 2010). In our model the energy content of relativistic protons that is necessary to reproduce the observed luminosity and brightness profile of the Coma radio halo is much smaller than that from calculations based on pure hadronic models that assume a similar magnetic field in the Coma cluster (Donnert et al 2010b), implying also a much smaller gamma-ray luminosity.

<sup>‡‡</sup> we assume an initial spectrum of protons  $N_p(p) = K_p p^{-2.6}$

<sup>§§</sup> more recently Donnert et al. (2010b) have shown that the observed steepening cannot be due to the SZ decrement due to the hot gas in the central Mpc region of the cluster

<sup>¶¶</sup> a similar conclusion comes from calculations of reacceleration of secondary particles in the Alfvénic case (Brunetti & Blasi 2005)

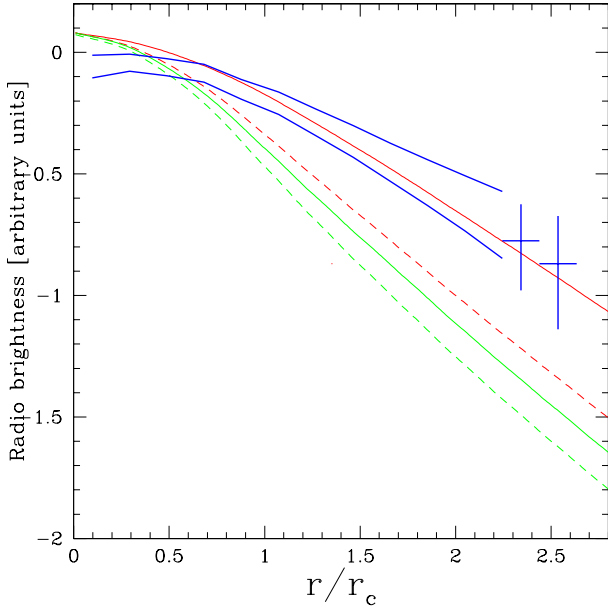


**Figure 6.** Radio brightness profile of the Coma radio halo (in arbitrary units). The observed profile (tick–blue lines and crosses) is taken from Govoni et al (2001) observations. Solid lines show the brightness profile at 330 MHz predicted by our reference model (red line) and by the model with lower magnetic field (green line). Dashed lines refer to the brightness profiles of both models (same color code) considering the case where turbulence is dissipated.

For seek of completeness, in Figure 5 (lower panels) we show the expected SED of the Coma cluster by assuming a magnetic field in the cluster 2.5 times smaller than that inferred from Bonafede et al.(2010) (see caption). In this case the properties of the Coma radio halo can be reproduced by assuming an energy content of relativistic protons  $E_{CR} \sim 25\%$  of the thermal energy, i.e. 7-8 times larger than that of our reference model, and the expected gamma ray emission increases significantly. Interestingly, in this case there would be a chance to detect the Coma cluster in the next years with the FERMI telescope.

Remarkably, on the other way round Figure 5 (lower panels) demonstrates the importance of present gamma ray upper limits: in the turbulent reacceleration picture, the magnetic field in the central regions of the Coma cluster cannot be significantly smaller than about  $2 \mu\text{G}$ , provided that hadronic collisions are the main source of the (seed) electrons in the cluster volume.

In the case of our reference model, the inverse Compton emission in the hard X-ray band is expected at a  $\sim$ percent level than the present Suzaku upper limit and a detection of the Coma cluster will be challenging even with the future hard X-ray experiments (e.g. ASTRO-H, Nustar). On the other hand, by assuming a magnetic field in the cluster 2.5 times smaller than that inferred from Bonafede et al.(2010) the expected inverse Compton emission increases significantly and there would be a chance to detect the Coma cluster with future hard X-ray telescopes. However, by assuming a magnetic field substantially smaller than that of our reference model, we find that the predicted radio profile is much steeper than the observed one (Fig. 6).

#### 4.3.2 Transient and long-living spectral components in galaxy clusters

In the context of our model the non-thermal emission from galaxy clusters is a mixture of two main spectral components : a *long-living* one that is emitted by the chain of secondary particles continuously generated by collisions between thermal and long-living (several Gyrs) relativistic protons, and a *transient* amplification of the SED that appears when relativistic particles are reaccelerated by the MHD turbulence generated (and then dissipated) in connection with cluster mergers (see also Brunetti et al 2009a); in this scenario the idea is that the *transient* synchrotron component generates the observed radio halos.

The non-thermal spectrum of dynamically relaxed galaxy clusters should be mainly due to the long-living spectral component. An example of this spectral component is shown in Figure 5 (dashed lines) where we report the synchrotron, inverse Compton and  $\pi^0$  emission calculated by assuming that MHD turbulence in the Coma cluster is dissipated.

The main effect of turbulent-reacceleration is to produce a amplification of the synchrotron (radio), inverse Compton (hard X) and  $\pi^0$  (gamma) emission in merging clusters (Fig. 5), while the effect of the dissipation of MHD turbulence in those clusters that become more relaxed is to suppress (only) the radio and the hard X-ray emission<sup>|||</sup>. Consequently in our model we expect a tight correlation between clusters dynamics and the radio (radio halos) and hard X-ray properties of galaxy clusters, but do not expect a tight correlation between gamma rays and cluster dynamics.

An important issue is the evolution of the radio halos in connection with cluster mergers and the difference between the radio properties of merging and relaxed clusters.

In the "classical" scenario, where turbulence reaccelerates primary electrons, the boosting of the synchrotron and hard X-ray emission during cluster mergers can be extremely large (eg. Fig. 5 in Brunetti et al 2009b; Fig. 6 in Casano 2010). Contrary to that, in our model the presence of relativistic protons in the IGM and the chain of secondary-particles decay induced by pp collisions put stringent constraints to the radio–evolution of galaxy clusters, since long–living spectral components are generated for about a Hubble time. Our calculations exploit this point and unveil the interplay between transient and long-living spectral components. In our model the boosting of the radio and hard X-ray luminosities due to reacceleration is fairly constrained, since it is essentially due to the reacceleration of secondary electrons from the energies where the injection spectrum of secondary electrons peaks (or from the energy where reacceleration is stronger than Coulomb losses) to the energies necessary to electrons to radiate synchrotron emission in the radio band (provided reacceleration is sufficient to accelerate particles up to these energies). This is  $\delta P/P \leq (EQ^\pm(E))_{E_l}/(EQ^\pm(E))_{E_h}$ , where  $E_l$  and  $E_h$  are about 100 MeV and 1 GeV respectively, that implies  $\delta P/P \sim 10 - 15$  for typical values of the slope of the proton spectrum,  $s = 2.4 - 2.8$ .

The predicted level of amplification and suppression of radio

<sup>|||</sup> Also the radial synchrotron profile in non–turbulent clusters is steeper than that in turbulent clusters (Fig. 6)

emission in galaxy clusters and its connection with cluster dynamics can be constrained by radio and X-ray observations. The recent radio follow up of a complete X-ray sample of galaxy clusters, the "GMRT Radio Halo Survey" (Venturi et al. 2007, 2008), leads to the discovery of a *bi-modal* behaviour of the clusters radio properties (Brunetti et al 2007, 2009b): radio halos are found in the most disturbed systems and trace the  $P_{1.4} - L_X$  correlation, on the other hand the majority of clusters are less disturbed and "radio quiet", with the limits to their radio luminosities about 10 times smaller than the radio luminosities of halos. As a matter of fact, our reacceleration model predicts that the level of the long-living synchrotron radiation in "radio quiet" clusters is similar to that of the upper limits from current GMRT radio observations, on the other hand the "classical" reacceleration scenario, where secondaries do not play a role, would predict a larger gap between radio halos and "radio quiet" clusters. Consequently future (deeper) radio observations may test the role of relativistic protons and secondary particles.

A second important issue is the possibility to detect gamma ray emission from galaxy clusters. In our reacceleration model gamma ray emission is a spectral component common in galaxy clusters, it essentially depends on the integrated merging history of clusters rather than to the dynamical status of a given cluster at the epoch of the observation; this is similar to classical hadronic models (eg., Blasi et al 2007 for review) and indeed our model evolves into these models when MHD turbulence in the IGM is dissipated. In our "reference" model-configuration we expect that gamma ray emission from galaxy clusters is difficult to detect in next years with present facilities. However, assuming a smaller magnetic field in the IGM, a larger number of relativistic protons must be assumed to explain radio halos and there is a chance to detect gamma rays from clusters in next years. As in the case of hadronic models, we expect that gamma ray emission scales with thermal properties as :

$$L_\gamma \propto \rho_{IGM}^2 MT \left\langle \frac{\epsilon_{CR}}{\epsilon_{th}} \right\rangle \quad (30)$$

where  $\langle \dots \rangle$  indicates emission weighted quantities in the cluster volume. In the most simple situation where we assume that  $\left\langle \frac{\epsilon_{CR}}{\epsilon_{th}} \right\rangle$  does not depend on cluster mass, Eq.30 implies a quasi linear scaling between gamma and (thermal) X-ray luminosities of galaxy clusters,  $L_\gamma \propto L_X^{1.3}$  (see also Pfrommer 2008 and Donnert et al 2010a for more detailed calculations based on cosmological simulations).

## 5 DISCUSSION AND CONCLUSIONS

If MHD turbulence is generated in galaxy clusters during massive merger events, relativistic protons can be reaccelerated enhancing the rate of generation of secondary particles in the IGM. Consequently, for a self-consistent treatment of the process, protons and their secondary products must be taken into account in the calculations of particle reacceleration by MHD turbulence in galaxy clusters.

\*\*\* Here we have considered  $L_X \propto \rho_{IGM}^2 M \sqrt{T}$ , and assumed the empirical scaling  $L_X \propto T^{2.98}$  (eg. Reiprich 2001).

In this paper we have assumed the picture of MHD turbulence in galaxy clusters as described in Brunetti & Lazarian (2007) to calculate the acceleration of primary protons and secondary particles by compressible MHD turbulence.

Upper limits to the gamma ray emission from galaxy clusters and radio upper limits to the cluster-scale synchrotron emission in clusters without radio halos constrain the energy density of relativistic protons in the central Mpc regions of galaxy clusters to less than a few percent of that of the IGM (Reimer et al 2004; Brunetti et al 2007, 2008; Aharonian et al 2009a,b; Ackermann et al 2010).

We have shown that a population of relativistic protons consistent with the above limits may be sufficient to generate the observed radio halos in merging clusters (including their observed brightness profiles and spectra) via the reacceleration of their secondary electrons by compressible MHD turbulence, provided that the spatial distribution of the relativistic protons is relatively flat and that the magnetic field in galaxy clusters is at the level derived from Rotation Measurements.

The main consequence of this theoretical scenario is that the non-thermal SED of galaxy clusters is given by the interplay of a transient component, generated by the reacceleration of secondary particles by MHD turbulence during cluster mergers (that generates radio halos), and a long-living component, that is generated by the secondary particles that are continuously injected by pp collisions in the IGM. In this case we expect a tight connection between radio halos and cluster mergers, as well as an amplification of the level of hard X-ray emission in merging clusters, while we expect no tight correlation between gamma rays and cluster dynamics. At the same time, we also expect that diffuse radio emission, due to secondary particles, must be common in galaxy clusters at a level that is about one order of magnitude below that of nowadays observed radio halos, i.e. at the same level of the upper limits derived by present radio observations of "radio quiet" clusters. This expectation can be tested by future (deeper) radio observations of "radio quiet" clusters. The level of gamma ray emission from nearby, massive, galaxy clusters is expected at about 10% of the level of present upper limits, assuming a magnetic field strength in these clusters in line with present studies of RM. This implies that only future telescopes (e.g. CTA) may lead to the detection of galaxy clusters in the gamma ray band. On the other hand, if the magnetic field in galaxy clusters is smaller, detection of galaxy clusters with FERMI could be possible in next years. In this respect, in the context of our model, present FERMI upper limits for the Coma cluster already provide a limit to the central value of the magnetic field  $B(0) \geq 1 - 2 \mu\text{G}$ .

### 5.1 Model simplifications and future steps

In our paper we focus on the role played by compressible MHD turbulence, essentially the fast modes. Our educated guess, motivated in Sect.2 and in Brunetti & Lazarian (2007), is that these modes are the most relevant for the reacceleration of relativistic particles in galaxy clusters. These modes were also identified as major scattering agent for Galactic cosmic rays (Yan & Lazarian 2002, 2004). The Alfvén modes and slow modes are not efficient for scattering if the turbulent energy is being injected at large

scales (Chandran 2000, Yan & Lazarian 2002). Their inefficiency stems from the both the spectra being steep in terms of parallel perturbations as well as fluctuations being very anisotropic (Goldreich & Sridhar 1995, Lazarian & Vishniac 1999, Cho & Vishniac 2000, Maron & Goldreich 2001, Cho, Lazarian & Vishniac 2002). If Alfvén modes are injected by instabilities they may have radically different properties from the modes of the large scale cascade. For instance, Alfvén modes arising from particle streaming have slab structure. Such waves efficiently interact with energetic particles. Other instabilities, e.g. gyroresonance one, can produce slab waves (see Gary 1993). The instabilities producing slab Alfvén modes may be induced by large scale compressible turbulence (see Lazarian & Beresnyak 2006). Indeed it is worth mentioning that the mode composition at smaller scales,  $l \ll l_A$ , in the IGM could become rather complex (e.g. Kato 1968; Eilek & Henriksen 1984).

To what extent our calculations are accurate depends on our understanding of properties of IGM turbulence. We assumed that the damping of fast modes with thermal particles can be obtained considering a collisionless plasma. At the same time, it can be argued (see e.g., Lazarian et al. 2010) that the degree of collisionality of astrophysical plasmas can be underestimated if only Coulomb collisions are taken into account, as particles in plasmas can interact through the mediation of the perturbed magnetic fields. The inevitable conclusion is that the collisionless formulae describing damping of these modes should be only applied to scales less than the mean free path, which is much shorter than the Coulomb mean free path. As a result, fast modes should be substantially less damped and be present on the scales which are much shorter than the earlier estimates, including those in this paper. The consequence of this is that a more appreciable portion of energy gets available for the acceleration of cosmic rays. Therefore, our present calculations may underestimate the efficiency of cosmic ray acceleration by turbulence. We plan to address the self-consistent problem elsewhere.

Following Brunetti & Lazarian (2007) in our paper we adopt quasi-linear-theory (henceforth QLT) to calculate particle acceleration by fast modes. In Brunetti & Lazarian (2007) we indeed have shown that for fast modes in the IGM it is  $\langle \omega \rangle \gg \langle \Gamma \rangle$ , where  $\langle \dots \rangle$  indicates angle-averaged quantities, that provides some justification to the use of QLT. More recent studies in Yan, Lazarian & Petrosian (2008) presented an approach to particle acceleration that generalizes the QLT and allows to take into account the effect of large scale variations of magnetic field. As numerical simulations which use the data from the actual MHD turbulence simulations (Beresnyak, Yan, Lazarian 2010) support the theory, we believe that, in future, going beyond the standard QLT approach may provide a more accurate description of the particle acceleration process, although we do not expect a large change (see Yan et al 2008).

Finally a unavoidable simplification in our semi-analytical calculations is that turbulence is homogeneous, in space and time, on the radio halo volume, during cluster mergers. On the other hand, cosmological numerical simulations of galaxy clusters show a more complex situation where intermittent and patchy large-scale turbulent motions are generated during multiple collisions between galaxy clusters (e.g. Vazza et al 2009a; Paul et al 2010). We believe

that to be more realistic one may need to vary the intensity of turbulence driving to describe different parts of galaxy clusters. Our idealized calculations of particle acceleration and evolution of compressible turbulence in the IGM provides a first step, implementing our formalism in detailed cluster-simulations is necessary to obtain a more reliable description of the morphology and spectral distribution of the non-thermal emission and of the connection between radio halos and cluster mergers.

## 5.2 A comparison with the Alfvénic approach

Earlier calculations of turbulent acceleration of primary protons and secondary electrons in galaxy clusters focus on the reacceleration by Alfvén modes (Brunetti & Blasi 2005). These studies first provided a description of the expected transient and long-living spectral components in galaxy clusters (e.g., Brunetti et al 2009a).

It is well known that the damping of these modes is mainly due to the interaction (gyro-resonance) with relativistic particles, that provides the main motivation to explore this possibility. On the other hand, as already mentioned, a complication of this approach is the anisotropy of Alfvén modes that develops when turbulence cascades from larger to smaller scales. Consequently in Alfvénic models the injection of Alfvén modes "directly" at small scales, i.e. comparable with the gyroradius of high energy particles, must be postulated, in which case it is also difficult to derive a overall picture connecting clusters mergers and the generation of these modes at such small scales.

A second issue in the modeling of Alfvénic acceleration of relativistic protons and of their secondary products is that the primary and secondary particles interact with Alfvén modes with different scales. This is because secondary electrons of energy  $E_e$  are mostly generated by collisions between higher energy protons,  $E_p \sim 10-50 \times E_e$ , and thermal targets that implies that these secondaries interact with modes on scales 10-50 times smaller than those of the parent primary protons (by consider the gyroresonant conditions  $k \sim eB/(cp \cos \theta)$ ). Consequently the ratio between the transient and long-living components in these models depends also on the spectrum of Alfvén modes. This implies a larger degree of freedom in Alfvénic models with respect to the more straightforward case treated in our paper where compressible MHD turbulence interact with relativistic particles.

## 5.3 Sources of primary electrons in a turbulent IGM

In general, if relativistic protons and electrons are present in the IGM, we expect that the MHD turbulence, generated during cluster mergers, would reaccelerate both these particles. If we assume an efficient confinement of cosmic rays in galaxy clusters, the unavoidable consequence of this scenario is that also the energy density of secondary products, due to pp collisions, should increase and consequently their contribution to the non-thermal clusters spectrum.

In our paper we have addressed this problem under the most extreme (and simplified) condition where only protons and their secondaries are present in the IGM; we note that un-



der these conditions the ratio of the energy densities of relativistic protons and of the emitting electrons in the IGM is maximized. In this context, we have shown that, assuming turbulent reacceleration at the level necessary to explain radio halos, the radio emission generated by secondary particles when turbulence is dissipated is consistent with present upper limits to the diffuse radio luminosity of clusters without radio halos. Also we have shown that the gamma-ray emission from the decay of secondary neutral-pions, that should be common in galaxy clusters and not tightly connected with their dynamical status, is expected at a level much smaller than that constrained from present upper limits with FERMI.

At the same time, however, under these conditions our calculations suggest that the difference between the cluster-scale radio emission of "turbulent" (merging) and "non-turbulent" (relaxed) clusters cannot be larger than about a factor ten, and that we expect to detect diffuse radio emission potentially in "all" massive clusters as soon as much deeper observations of clusters that are presently defined "radio-quiet" will become available.

On the other hand primary relativistic electrons should be present, at some level, in the IGM. It is well known that active radio galaxies may fill large volumes in the IGM with relativistic plasma, relativistic electrons age rapidly but they can be accumulated at hundred MeV energies for longer times, especially in the external regions (Fig.1). Other sources of relativistic primary electrons that are usually considered in the literature are Galactic Winds and Starburst galaxies (e.g., Völk & Atoyan 1999) and shock waves (e.g., Ensslin et al 1998; Sarazin 1999; Ryu et al 2003; Pfrommer et al. 2006; Skillman et al 2008; Vazza et al 2009b), evidence for the latter process come from the observations of radio relics that indeed suggest a connection between shocks and electron acceleration (or reacceleration) in the IGM (e.g., Markevitch et al 2005 and Giacintucci et al 2008 for observations of a shocks-relics connection in clusters).

In addition to these processes, another possibility that requires more attention is that the primary electrons can be "created" in the IGM. Magnetic reconnection presents a natural way for doing this, as electrons bounces back and forth between converging magnetic fluxes can gain energy through the first order Fermi acceleration (Gouveia dal Pino & Lazarian 2003). Although it is generally believed that reconnection is a slow process, potentially turbulence can significantly enhance the reconnection rate (Lazarian & Vishniak 1999). Exploring this mechanism and its interplay with particle reacceleration by MHD turbulence in the IGM may open new perspective in our understanding of non-thermal cluster-scale emission and of its connection with cluster mergers. We aim to discuss in detail this point in a future paper, yet for completeness here we dedicate an Appendix to turbulent reconnection.

The presence of primary electrons in the IGM may significantly affect the SED of galaxy clusters and its evolution. In particular if the number density of primary electrons is comparable to (or larger than) that of secondary particles, a smaller number of relativistic protons is required by the our model to match the observed spectrum of radio halos. This has an impact on the expected gamma ray emission from galaxy clusters that would be consequently smaller than that expected from the calculations presented in Sect.4.3. A sec-

ond important point is that if a population of reaccelerated primary electrons significantly contributes to the observed radio halo emission, the expected ratio between transient and long living components in the radio and hard X-ray bands increases with respect to that derived in Sect.4.3. As a matter of fact, assuming that primary electrons are dominant with respect to secondaries our picture evolves into the "classical" reacceleration model (eg., Brunetti et al 2001, 2004; Petrosian 2001; Cassano & Brunetti 2005) where indeed the luminosity of giant radio halos is suppressed by several orders of magnitude when galaxy clusters evolve into relaxed systems (e.g. Brunetti et al 2009b; Cassano 2010). Consequently, we believe that future gamma ray and radio observations will be crucial also to constrain the ratio of primary and secondary electrons in the IGM.

## 6 ACKNOWLEDGMENTS

We thank the anonymous referee for useful comments. We acknowledge grants from INAF (PRIN-INAF2007 and 2008), ASI-INAF (I/088/06/0), NSF (AST 0808118) and NASA (NNX09AH78G) and support by the NSF Center for Magnetic Self-Organization. GB thanks the Dep. of Astronomy of Wisconsin University at Madison and the Harvard-Smithsonian Center for Astrophysics for hospitality.

## REFERENCES

- Ackermann M., et al. 2010, ApJ 717, L71  
 Ajello M., Rebusco P., Cappelluti N., Reimer O., Böhringer H., Greiner J., Cehrels N., Tueller J., Moretti A., 2009, ApJ 690, 367  
 Aleksic J., et al 2010, ApJ 710, 634  
 Aharonian F.A., et al., 2009a, A&A 495, 27  
 Aharonian F.A., et al., 2009b, A&A 502, 437  
 Badhwar G.D, Golden R.L., Stephens S.A., 1977, Phy.Rev.D 15, 820  
 Beresnyak A., Lazarian A., 2008, ApJ 682, 1070  
 Beresnyak A., Lazarian A., 2009, ApJ 702, 460  
 Beresnyak A., Lazarian A., 2010, arXiv:1002.2428  
 Beresnyak A., Yan H., Lazarian A., 2010, arXiv:1002.2646  
 Beresnyak A., Jones T.W., Lazarian A., 2009, ApJ 707, 1541  
 Berezhinsky V.S., Blasi P., Ptuskin V.S., 1997, ApJ 487, 529  
 Berrington R., Dermer C.D., 2003, ApJ 594, 709  
 Blasi P., 2001, APh 15, 223  
 Blasi P., Colafrancesco S., 1999, APh 12, 169  
 Blasi P., Gabici S., Brunetti G., 2007, IJMPA 22, 681  
 Bonafede A., Feretti L., Murgia M., Govoni F., Giovannini G., Dallacasa D., Dolag K., Taylor G.B., 2010, A&A 513, 30  
 Briel U.G., Henry J.P., Böhringer H., 1992, A&A 259, L31  
 Brunetti G., 2009, A&A 508, 599  
 Brunetti G., Setti G., Feretti L., Giovannini G., 2001, MNRAS 320, 365  
 Brunetti G., Blasi P., Cassano R., Gabici S., 2004, MNRAS 350, 1174  
 Brunetti G., Blasi P., 2005, MNRAS 363, 1173  
 Brunetti G., Lazarian A., 2007, MNRAS 378, 245  
 Brunetti G., Venturi T., Dallacasa D., Cassano R., Dolag K., Giacintucci S., Setti G., 2007, ApJ 670, L5  
 Brunetti G., Giacintucci S., Cassano R., Lane W., Dallacasa D., Venturi T., Kassim N.E., Setti G., Cotton W.D., Markevitch M., 2008, Nature 455, 944  
 Brunetti G., Blasi P., Cassano R., Gabici S., 2009a, AIPC 1112, 129



- Brunetti G., Cassano R., Dolag K., Setti G., 2009b, *A&A* 507, 661
- Cassano R., 2009, *ASPC* 407, 223
- Cassano R., 2010, arXiv:1004.1171
- Cassano R., Brunetti G., 2005, *MNRAS* 357, 1313
- Cassano R., Brunetti G., Setti G., Govoni F., Dolag K., 2007, *MNRAS* 378, 1565
- Chandran B.D.G., 2000, *Phys. Rev. Lett.*, 85, 4656
- Chandran B.D.G., 2008, *ApJ* 685, 646
- Cho J., Vishniac E., 2000, *ApJ* 539, 273
- Cho J., Lazarian A., 2002, *ApJ* 575, L63
- Cho J., Lazarian A., Vishniac E.T., 2002, *ApJ* 564, 291
- Cho J., Lazarian A., 2003, *MNRAS* 345, 325
- Cho J., Lazarian A., 2005, *ThCFD* 19, 127
- Ciaravella A., Raymond J.C., 2008, *ApJ* 686, 1372
- Clarke T.E., Kronberg P.P., Böhringer H., 2001, *ApJ* 547, L111
- David L.P., Slyz A., Jones C., Forman W., Vrtilik S.D., Arnaud K.A., 1993, *ApJ* 412, 479
- de Gouveia dal Pino E.M., Lazarian A., 2003, astro-ph/030705
- de Gouveia dal Pino E.M., Lazarian A., 2005, *A&A* 441, 845
- Dennison B., 1980, *ApJ* 239L
- Dermer C.D., 1986a, *ApJ* 307, 47
- Dermer C.D., 1986b, *A&A* 157, 223
- Dolag K., Ensslin T.A., 2000, *A&A* 362, 151
- Dolag K., Bartelmann M., Lesch H., 2002, *A&A* 387, 383
- Dolag K., Grasso D., Springel V., Tkachev I., 2005, *JCAP* 1, 9
- Donnert J., Dolag K., Cassano R., Brunetti G., 2010a, arXiv:1003.0336
- Donnert J., Dolag K., Brunetti G., Cassano R., Bonafede A., 2010b, *MNRAS* 401, 47
- Drake J.F., Swisdak M., Che H., Shay M.A., 2006, *Nature* 443, 553
- Drake J.F., Opher M., Swisdak M., Chamoun J., 2010, *ApJ* 709, 963
- Eilek J.A., 1979, *ApJ* 230, 373
- Eckert D., Neronov A., Courvoisier T.J.-L., Produit N., 2007, *A&A* 470, 835
- Ensslin T.A., Wang Y., Nath B.B., Biermann P.L., 1998, *A&A* 333, L47
- Ensslin T.A., Pfrommer C., Springel V., Jubelgas M., 2007, *A&A* 473, 41
- Feretti L., 2002, *IAUS* 199, 133
- Ferrari, C.; Govoni, F.; Schindler, S.; Bykov, A. M.; Rephaeli, Y., 2008, *SSRv* 134, 93
- Fisk L.A., 1976, *Journal of Geophys. Research* 81, 4633
- Fujita Y., Takizawa M., Sarazin C.L., 2003, *ApJ* 584, 190
- Fusco-Femiano R., dal Fiume D., Feretti L., Giovannini G., Grandi P., Matt G., Molendi S., Santangelo A., 1999, *ApJ* 513, L21
- Fusco-Femiano R., Orlandini M., Brunetti G., Feretti L., Giovannini G., Grandi P., Setti G., 2004, *ApJ* 602, L73
- Gabici S., Blasi P., 2003, *ApJ* 583, 695
- Gary S.P., 1993, in *Theory of Space Plasma Microinstabilities*, pp. 193, Cambridge University Press
- Giacintucci S., Venturi T., Macario G., Dallacasa D., Brunetti G., Markevitch M., Cassano R., Bardelli S., Athreya R., 2008, *A&A* 486, 347
- Giovannini G., Feretti L., Venturi T., Kim K.-T., Kronberg P.P., 1993, *ApJ* 406, 399
- Goldreich P., Sridhar S.: 1995, *ApJ* 438, 763
- Govoni F., 2006, *AN* 327, 539
- Govoni F., Ensslin T.A., Feretti L., Giovannini G., 2001, *A&A* 369, 441
- Higdon J.C., 1984 *ApJ* 285, 109
- Hoefl, M. & Brueggen, M. 2007, *MNRAS* 375, 77
- Hwang C.-Y., 2004, *JKAS* 37, 461
- Kowal G., Lazarian A., 2010, arXiv:1003.3697
- Lazarian A., 2005, *AIPC* 784, 495
- Lazarian A., 2006a, *AN* 327, 609
- Lazarian A., 2006b, *ApJ* 645, L25
- Lazarian A., Vishniac E.T., 1999, *ApJ* 517, 700
- Lazarian A., Beresnyak A., 2006, *MNRAS* 373, 1195
- Lazarian A., Opher M., 2009, *ApJ* 703, L8
- Lazarian A., Desiati, 2010, *ApJ* submitted
- Lazarian A., Kowal G., Vishniac E., Kulpa-Dubel K., Otmianowska-Mazur K., 2010, arXiv:1003.2656
- Lithwick Y., Goldreich P., 2001, *ApJ* 562, 279
- Liu C.S., Mok Y., 1977, *Phys. Rev. Letters* 38, 162
- Lutovinov A.A., Vikhlinin A., Churazov E.M., Revnivtsev M.G., Sunyaev R.A., 2008, *ApJ* 687, 968
- Macario G., Venturi T., Brunetti G., Dallacasa D., Giacintucci S., Cassano R., Bardelli S., Athreya R., 2010, arXiv:1004.1515
- Markevitch M., Govoni F., Brunetti G., Jerius D., 2005, *ApJ* 627, 733
- Maron J., Goldreich P., 2001, *ApJ* 554, 1175
- Matthaeus W.H., Zhou Y., 1989, *PhFlB* 1, 1929
- Matthaeus W.H., Lamkin S.L., 1985, *PhFl* 28, 303
- Matthaeus W.H., Lamkin S.L., 1986, *PhFl* 29, 2513
- Melrose D.B., 1968, *ApSS* 2, 171
- Miller J.A., La Rosa T.N., Moore R.L., 1996, *ApJ* 461, 445
- Miniati F., Jones T.W., Kang H., Ryu D., 2001, *ApJ* 562, 233
- Moghaddam-Taaheri E., Vlahos L., Rowland H.L., Papadopoulos K., 1985, *Phys. of Fluids* 28, 3356
- Montgomery D., Turner L., 1981, *PhFl* 24, 825
- Moskalenko I.V., Strong A.W., 1998, *ApJ* 493, 694
- Paesold G., Benz A.O., 1999, *A&A* 351, 741
- Parker E.N., 1957, *JGR* 62, 509
- Paul S., Iapichino L., Miniati F., Bagchi J., Mannheim K., 2010, arXiv:1001.1170
- Perez J.C., Boldyrev S., 2009, *PhRvL* 102, 025003
- Perkins, J.S., 2008, *AIPC* 1085, 569
- Petrosian V., 2001, *ApJ* 557, 560
- Petrosian V., East W.E., 2008, *ApJ* 682, 175
- Petscheck H.E., 1964, *NASSP* 50, 425
- Pilipp W., Völk H.J., 1971, *Journal of Plasma Phys.* 6, 1
- Pfrommer C., Ensslin T.A., 2004, *MNRAS* 352, 76
- Pfrommer C., Springel V., Ensslin T.A., Jubelgas M., 2006, *MNRAS* 367, 113
- Pfrommer C., 2008, *MNRAS* 385, 1242
- Reimer A., Reimer O., Schlickeiser R., Iyudin A., 2004, *A&A* 424, 773
- Reimer O., Pohl M., Sreekumar P., Mattox J.R., 2003, *ApJ* 588, 155
- Reiprich T.H., 2001, astro-ph/0308137
- Rephaeli Y., Gruber D., Blanco P., 1999, *ApJ* 511, L21
- Ricker P.M., Sarazin C.L., 2001, *ApJ* 561, 621
- Rossetti M., Molendi S., 2004, *A&A* 414, L41
- Roettiger K., Burns J.O., Loken C., 1996, *ApJ* 473, 651
- Roettiger K., Loken C., Burns J.O., 1997, *ApJS* 109, 307
- Ryu, D., Kang, H., Hallman, E., & Jones, T.W. 2003, *ApJ* 593, 599
- Ryu D., Kang H., Cho J., Das S., 2008, *Science* 320, 909
- Sarazin, C.L. 1999, *ApJ* 520, 529
- Schekochihin A.A., Cowley S.C., Kulsrud R.M., Hammett G.W., Sharma P., 2005, *ApJ* 629, 139
- Schekochihin A.A., Cowley S.C., Rincon F., Rosin M.S., 2010, *MNRAS* 405, 291
- Schlickeiser R., Sievers A., Thiemann H.: 1987, *A&A* 182, 21
- Schlickeiser R., Miller J.A., 1998, *ApJ* 492, 352
- Schlickeiser R., 2002, *Cosmic Ray Astrophysics*, Springer-Verlag, Berlin Heidelberg
- Shebalin J.V., Matthaeus W.H., Montgomery D., 1983, *JPlPh* 29, 525
- Skillman S.W., O'Shea B.W., Hallman E.J., Burns J.O., Norman M.L., 2008, *ApJ* 689, 1063
- Speiser T.W., 1970, *P&SS* 18, 613
- Stecker F.W., 1970, *Ap&SS* 6, 377

Steinacker J., Miller J.A., 1992, ApJ 393, 764  
 Stephens S.A., Badhwar G.D., 1981, Ap&SS 76, 213  
 Strauss H.R., 1988, ApJ 326, 412  
 Subramanian K., Shukurov A. Haugen N.E.L., 2006, MNRAS 366, 1437  
 Sunyaev R.A., Norman M.L., Bryan G.L., 2003, Astron. Lett. 29, 783  
 Sweet P.A., 1958, IAUS 6, 123  
 Thierbach M., Klein U., Wielebinski R., 2003, A&A 397, 53  
 Vazza F., Tormen G., Cassano R., Brunetti G., Dolag K., 2006, MNRAS 369, L14  
 Vazza F., Brunetti G., Kritsuk A., Wagner R., Gheller C., Norman M., 2009a, A&A 504, 33  
 Vazza F., Brunetti G., Gheller C., 2009b, MNRAS 395, 1333  
 Venturi, T., Giacintucci, S., Brunetti, G., Cassano, R., Bardelli, S., Dallacasa, D., & Setti, G. 2007, A&A 463, 937  
 Venturi T., Giacintucci S., Dallacasa D., Cassano R., Brunetti G., Bardelli S., Setti G., 2008, A&A 484, 327  
 Völk H.J., Aharonian F.A., Breitschwerdt D., 1996, SSRv 75, 279  
 Völk H.J., Atoyan A.M., 1999, APh 11, 73  
 Yan H., Lazarian A., 2002, Phys. Rev. Lett. 89, 1102  
 Yan H., Lazarian A., 2004, ApJ 614, 757  
 Yan H., Lazarian A., Petrosian V., 2008, ApJ 684, 1461  
 Wik D.R., Sarazin C.L., Finoguenov A., Matsuchita K., Nakazawa K., Clarke T.E., 2009, ApJ 696, 1700  
 Willson M.A.G., 1970, MNRAS 151, 1  
 ZuHone J., 2010, arXiv:1004.3820

## 7 APPENDIX: MAGNETIC FIELD RECONNECTION AS SOURCE OF PRIMARY ELECTRONS IN THE IGM

Magnetic reconnection is an ubiquitous process in magnetized flows, expected to happen when magnetic fields of non-parallel direction get into contact. However, the textbook processes of magnetic reconnection seem to fall short of providing the desired solution. The Sweet-Parker reconnection (Sweet 1958, Parker 1957) is too slow. The speed of the reconnection scales as Alfvén velocity  $v_A$  times the inverse value of the square root of the Lundquist number  $S^{1/2} \equiv (Lv_A/\eta)^{1/2}$ , where  $L$  is the size of the magnetic regions and  $\eta$  is magnetic diffusivity. As Lundquist number can be for the IGM  $10^{15}$  and higher, it is clear that the Sweet-Parker reconnection can handle only a negligible fraction of magnetic flux in the Hubble time. Petschek proposed a solution where magnetic fields get into contact at a sharp angle (Petschek 1964).

In the Petschek model no efficient acceleration of particles is expected at reconnection sites. Indeed the traditional processes of acceleration which rely on the electric field in the reconnection region are inefficient, as the reconnection region is too small and releases only a small portion of magnetic energy. Slow shocks predicted in the Petschek model are likely to be inefficient for the particle acceleration (see discussion in Beresnyak, Jones & Lazarian 2009). In addition, observational data does not support the X-point reconnection predicted in the Petschek model either (see Ciaravella & Raymond 2008).

A shortcoming of many discussions of magnetic reconnection is that the traditional setup does not include ubiquitous pre-existing astrophysical turbulence. As turbulence radically changes many astrophysical processes, the influence of turbulence on reconnection has attracted the atten-

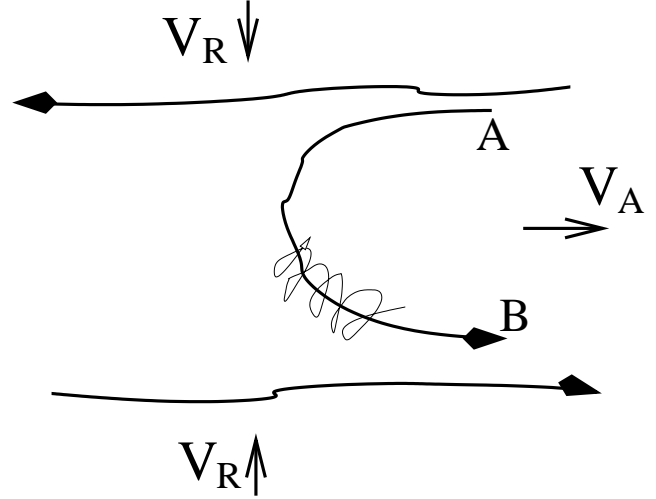


**Figure 7.** Cosmic rays entrained over a shrinking loop of reconnected magnetic flux bounce between points A and B and gain energy (from Lazarian 2005).

tion of researchers for a long time (see Speizer 1970; Mathaeus & Lamkin 1985, 1986; Strauss 1988).

A new approach to the effects of turbulence was adopted in Lazarian & Vishniac (1999, henceforth LV99). This model predicts reconnection speeds close to the turbulent velocity in the fluid. More precisely, assuming isotropically driven turbulence characterized by an injection scale,  $l$ , smaller than the current sheet length  $L$ , LV99 obtained :

$$V_{rec} \approx v_A (l/L)^{1/2} (V_i/v_A)^2, \quad (31)$$

where the turbulent injection velocity  $V_i$  is assumed to be less than  $v_A$ . If  $L < l$ , the first factor in Eq. (31) should be changed to  $(L/l)^{1/2}$  (LV99). If turbulent injection velocity is larger than  $v_A$  the reconnection happens at the Alfvén speed for  $L > l_A$ . For  $L < l_A$  a factor  $(L/l_A)^{1/2}$  should substitute the factor of  $(l/L)^{1/2}$  in Eq. (31). Physically this reflects the fact that at sufficiently small scales magnetic field energy dominates the kinetic energy and the magnetic field lines get only weakly perturbed by turbulent motions. Figure 7 provides the simplest realization of the acceleration of particles within the reconnection region expected within LV99 model. As a particle bounces back and forth between converging magnetic fluxes, it gains energy through the first order Fermi acceleration (de Gouveia dal Pino & Lazarian 2003, 2005; see also Lazarian 2005). The first order acceleration of particles entrained on contracting magnetic loop can be understood from the Liouville theorem, i.e the preservation of the phase volume which includes the spatial and momentum coordinates. As in the process of reconnection the magnetic tubes are contracting and the configuration space presented by magnetic field shrinks, the regular increase of the particle’s energies is expected. The requirement for the process to proceed efficiently is to keep the accelerated particles within the contracting magnetic loop. This introduces limitations on the particle diffusivities perpendicular to magnetic field direction. Thus high perpendicular diffusion of particles may decouple them from the magnetic field. Indeed, it is easy to see that while the particles within a magnetic flux rope depicted in Figure 7 bounce back and

forth between the converging mirrors and get accelerated, if these particles leave the flux rope fast, they may start bouncing between the magnetic fields of different flux ropes which may sometimes decrease their energy. Thus it is important that the particle diffusion parallel and perpendicular magnetic field stays different. Particle anisotropy which arises from particle preferentially getting acceleration in terms of the parallel momentum may also be important. The energy spectrum was derived in GL03 :

$$N(E)dE = C \cdot E^{-5/2} dE, \quad (32)$$

In Drake et al. (2006) this idea was enriched by taking into account the backreaction of particles.

We believe that such an acceleration can be present in IGM. Two dimensional numerical simulations of acceleration can be found in Drake et al. (2006, 2010) and first three dimensional simulations were presented in Lazarian et al. (2010). In typical IGM the small scale reconnection of turbulent field should be collisionless and during this collisionless with electrons and ions decoupled. This should enable the acceleration of electrons. The idea of particle acceleration in reconnection regions was recently applied to describe anomalous cosmic ray acceleration in Heliosphere (Lazarian & Opher 2009, Drake et al.2010) and acceleration of cosmic rays in heliotail (Lazarian & Desiati 2010). In IGM magnetic turbulence creates magnetic reversals and therefore we expect to see additional sources of energetic electrons. In terms of the model that we discuss the electron acceleration in magnetic reconnection sites should increase the energy density of electrons and modify their spectrum. We shall discuss these effects elsewhere.